J. Math. Anal. Appl. 475 (2019) 1883–1909

Contents lists available at ScienceDirect

Journal of Mathematical Analysis and Applications

www.elsevier.com/locate/jmaa

Pattern formation for a two-dimensional reaction-diffusion model with chemotaxis

Manjun Ma [a,*], Meiyan Gao [b], R. Carretero-González [c,d,e]

[a] *Department of Mathematics, School of Sciences, Zhejiang Sci-Tech University, Hangzhou, Zhejiang, 310018, China*
[b] *Department of Mathematics, College of Sciences, China Jiliang University, Hangzhou, Zhejiang, 310018, China*
[c] *Nonlinear Dynamical Systems Group, USA* [1]
[d] *Computational Science Research Center, USA* [2]
[e] *Department of Mathematics and Statistics, San Diego State University, San Diego, CA 92182-7720, USA*

ARTICLE INFO

Article history:
Received 2 October 2017
Available online 27 March 2019
Submitted by J. Shi

Keywords:
Pattern formation
Amplitude equation
Chemotaxis
Weakly nonlinear analysis

ABSTRACT

This paper is devoted to study the formation of stationary patterns for a chemotaxis model with nonlinear diffusion and volume-filling effect over a bounded rectangular domain. By using linear stability analysis around the homogeneous steady states we establish conditions for the existence of unstable mode bands that lead to the formation of spatial patterns. We derive the Stuart-Landau equations for the pattern amplitudes by means of weakly nonlinear multiple scales analysis and Fredholm theory. In particular, we find asymptotic expressions for a wide range of patterns sustained by the system. These patterns include mixed-mode, square, hexagonal, and roll stationary configurations. Our analytical results are corroborated by direct simulations of the underlying chemotaxis system.

1. Introduction and preliminaries

Pattern formation in nature involves a series of complex processes. For instance, the pattern formation mechanisms involved in morphogenesis have not been completely understood. Significant progress toward this direction was made in 1952 by Alan Turing in [20] where he put forward that diffusion was one of main ingredients behind the spontaneous emergence of ordered structures (called patterns) in a variety of non-equilibrium systems. Since then, self-organized patterning in reaction-diffusion systems driven by diffusion has been extensively studied. Such systems include, but are not limited to, the Gierer-Meinhardt

* Corresponding author.
E-mail address: mjunm9@zstu.edu.cn (M. Ma).
[1] http://nlds.sdsu.edu.
[2] http://www.csrc.sdsu.edu.

https://doi.org/10.1016/j.jmaa.2019.03.060

model [6], the Sel'kov model [10,21], the predator-prey model with cross-diffusion [1,2,18], the Brusselator model with nonlinear diffusion [3–5], the chemotaxis model [7,9,11,13,16,22,26], and references therein.

In this work, we are interested in investigating the pattern formation for the following two-dimensional chemotaxis system with nonlinear diffusion and volume-filling effect:

$$\begin{cases} u_t = \nabla \cdot (D(1-u)^{-\alpha}\nabla u - \chi u(1-u)^{\beta}\nabla v) + \mu u\left(1 - \dfrac{u}{u_c}\right), & \mathbf{x} \in \Omega,\ t > 0, \\ v_t = \Delta v - v + u, & \mathbf{x} \in \Omega,\ t > 0, \\ \nabla u \cdot \nu = \nabla v \cdot \nu = 0, & \mathbf{x} \in \partial\Omega,\ t > 0, \\ u(\mathbf{x}, 0) = u_0(\mathbf{x}), v(\mathbf{x}, 0) = v_0(\mathbf{x}), & \mathbf{x} \in \Omega, \end{cases} \tag{1.1}$$

where $u(\mathbf{x}, t)$ is the cell density and $v(\mathbf{x}, t)$ denotes the concentration of chemical produced by the cells. The domain is chosen as $(\mathbf{x}, t) \in \Omega \times [0, +\infty)$ with $\mathbf{x} = (x, y) \in \Omega = (0, l_x) \times (0, l_y)$ and $l_x, l_y > 0$, and $\partial\Omega$ represents the boundary of Ω. The vector ν denotes the outward unit normal vector on $\partial\Omega$. The cell density dependent term $D(1-u)^{-\alpha}$ corresponds to (nonlinear) diffusion with strength $D > 0$. The function $u(1-u)^{\beta}$ describes the chemotactic sensitivity where the number 1 is the normalized *crowding capacity* which is the maximal number that an unit volume of space can accommodate cells. The real parameters α and β, controlling the level of nonlinearity for the diffusion and chemotactic sensitivity terms, are constants such that $\alpha + \beta > 1$ (see below). Finally, the parameter $\mu > 0$ corresponds to the intrinsic growth rate of cells, $\chi > 0$ is the so-called chemotactic coefficient, and u_c corresponds to the *carrying capacity* of the system.

The system (1.1) is a generalized form of the volume-filling chemotaxis model which was firstly introduced by Painter and Hillen [16]. We refer readers to Wang [24,25] or Wang et al. [26] for the detailed derivation of Eq. (1.1). Sufficient conditions for the existence and the non-existence of non-constant steady states of Eq. (1.1) have been established in [12]. The existence of the global solution, global structures of the steady states bifurcating from the constant steady states, and their stability have been investigated in [11]. In [15] the authors theoretically and numerically established that patterns for system (1.1) propagate, in a large and one-dimensional spatial domain, as traveling waves. In [14] the authors showed that, when ignoring the geometry of the domain, chemotaxis is the key mechanism for pattern formation and presented analytical expressions for pattern formation in a one-dimensional domain. Owing to these results, we assume all throughout the manuscript that

$$0 < u_c < 1,\ \alpha + \beta > 1, \quad \alpha, \beta \in \mathbb{R}, \tag{1.2}$$

and when referring to system (1.1), initial data (u_0, v_0) always satisfies

$$(u_0, v_0) \in [\mathcal{W}^{1,\infty}(\Omega)]^2 \text{ and } 0 \le u_0(\mathbf{x}) < 1,\ v_0(\mathbf{x}) \ge 0,\ \mathbf{x} \in \overline{\Omega}, \tag{1.3}$$

where $\mathcal{W}^{1,\infty}(\Omega)$ is the Sobolev space with ∞-norm defined by $||\cdot||_{1,\infty} = \operatorname{ess\,sup}_{x\in\Omega}(|\cdot| + |\nabla\cdot|)$ and $\overline{\Omega} \equiv \Omega \cup \partial\Omega$. The conditions (1.2) and (1.3) guaranty that the system (1.1) is globally well posed. Furthermore, any steady states $(u(x), v(x))$ are bounded as $0 < (u(x), v(x)) < 1$ in Ω.

The present manuscript aims to obtain the analytical expressions of patterns in a two-dimensional domain by employing Fredholm theory and weakly nonlinear analysis with multiple temporal scales. All the obtained analytical results will be compared with the corresponding full numerical solutions of the original system. Our presentation is structured as follows. In Section 2 we give the interval of unstable modes and the sufficient conditions for the existence of linear spatio-temporal patterns. In Section 3 we establish the formulae for stationary patterns for each of the cases under study: single and mixed-mode patterns, rolls, square and hexagonal patterns. Full numerical solutions of the original system are also carried out to corroborate the results of our weakly nonlinear multiple scales analysis. Finally, in Section 4 we conclude our work and bring forward problems for further study.

2. Instability modes and linear patterns

In this section we present the conditions for pattern formation in system (1.1). To proceed, we first recall some results on the eigenvalue problem for the two-dimensional negative Laplace operator:

$$\begin{cases} -\Delta\omega = \lambda\omega, \quad (x,y) \in (0,l_x) \times (0,l_y), \\ \dfrac{\partial\omega}{\partial x}(0,y) = \dfrac{\partial\omega}{\partial x}(l_x,y) = 0, \quad 0 < y < l_y, \\ \dfrac{\partial\omega}{\partial y}(x,0) = \dfrac{\partial\omega}{\partial y}(x,l_y) = 0, \quad 0 < x < l_x. \end{cases} \tag{2.1}$$

The problem (2.1) has eigenvalues

$$\lambda = \lambda_{mn} = \lambda_m + \lambda_n = \left(\frac{m\pi}{l_x}\right)^2 + \left(\frac{n\pi}{l_y}\right)^2 \tag{2.2}$$

with corresponding eigenfunctions

$$\omega_{mn}(x,y) = \cos\frac{m\pi x}{l_x}\cos\frac{n\pi y}{l_y}, \tag{2.3}$$

where $m, n = 0, 1, 2, \ldots$. Now, focusing on system (1.1), it is straightforward to check that it has two homogeneous steady states $\omega_0 = (0,0)$ and $\omega_c = (u_c, u_c)$. Using linear stability analysis, it is straightforward to show that ω_0 is always unstable. In what follows we opt to ignore this (trivial) unstable equilibrium and choose to focus our study of pattern formation on the nontrivial homogeneous state ω_c. Linearizing the system (1.1) about ω_c yields

$$\begin{cases} \dfrac{\partial W}{\partial t} = \mathcal{K}(\chi)W, \quad (x,y) \in (0,l_x) \times (0,l_y), \quad t > 0, \\ \dfrac{\partial W}{\partial \nu} = 0, \quad x = 0, l_x;\ y = 0, l_y, \quad t > 0, \end{cases} \tag{2.4}$$

with

$$W = \begin{pmatrix} u - u_c \\ v - u_c \end{pmatrix}, \tag{2.5}$$

and

$$\mathcal{K}(\chi) = \begin{pmatrix} D(1-u_c)^{-\alpha}\Delta - \mu & -\chi u_c(1-u_c)^{\beta}\Delta \\ 1 & \Delta - 1 \end{pmatrix}. \tag{2.6}$$

We seek for solutions of system (2.4) with zero Neumann boundary conditions in the form of plane waves $e^{i\mathbf{k}\cdot\mathbf{x}+\rho t}$, where $\mathbf{k}$ is the wave vector with magnitude

$$k^2 = |\mathbf{k}|^2 = \left(\frac{m\pi}{l_x}\right)^2 + \left(\frac{n\pi}{l_y}\right)^2, \tag{2.7}$$

associated with (2.2)–(2.3), where ρ is the temporal growth rate depending on k^2. Substituting these plane wave solutions into the system (2.4) yields the dispersion relation

$$\rho^2 + p(k^2)\rho + q(k^2) = 0, \tag{2.8}$$

where

$$p(k^2) = [D(1-u_c)^{-\alpha} + 1]k^2 + 1 + \mu, \tag{2.9}$$

$$q(k^2) = D(1-u_c)^{-\alpha}k^4 + \left[D(1-u_c)^{-\alpha} + \mu - \chi u_c(1-u_c)^{\beta}\right]k^2 + \mu. \tag{2.10}$$

Obviously, $p(k^2) > 0$, thus it is impossible for the steady state ω_c to undergo a Hopf bifurcation. For the emergence of spatial patterns, it is sufficient that there exists at least a wave number k such that $\mathrm{Re}(\rho) > 0$. This instability condition can be satisfied for all $k \neq 0$ for which $q(k^2) < 0$. Then, we have the following straightforward result:

Proposition 2.1. *Let D, μ, u_c, α and β be fixed, and*

$$\chi_c = \frac{(\sqrt{D(1-u_c)^{-\alpha}} + \sqrt{\mu})^2}{u_c(1-u_c)^{\beta}}. \tag{2.11}$$

Then, the following statements are true.

- (P_1) *If $\chi = \chi_c$: the steady state ω_c is neutrally stable and thus χ_c is called the critical value for chemotaxis at which*

$$k = \left(\frac{\mu}{D(1-u_c)^{-\alpha}}\right)^{1/4} \equiv k_c \tag{2.12}$$

  such that $\min q(k^2) = q(k_c^2) = 0$, and k_c is the critical value for the wave number.
- (P_2) *If $\chi > \chi_c$: the steady state ω_c is unstable and there exists an interval of unstable wave numbers (k_1^2, k_2^2) where $q(k^2) < 0$ and $q(k_i^2) = 0, i = 1, 2$ with*

$$k_1^2 = \frac{1}{2D}\left(\eta - \sqrt{\eta^2 - 4\mu D(1-u_c)^{\alpha}}\right), \quad k_2^2 = \frac{1}{2D}\left(\eta + \sqrt{\eta^2 - 4\mu D(1-u_c)^{\alpha}}\right)$$

  and

$$\eta = \chi u_c(1-u_c)^{\alpha+\beta} - \mu(1-u_c)^{\alpha} - D > 0.$$

- (P_3) *Suppose $\chi > \chi_c$. If at least one mode $k \in (k_1^2, k_2^2)$ is admissible for the domain and the zero Neumann boundary conditions, then a spatial pattern must appear.*

From Eqs. (2.1)–(2.3), the generalized form for solutions to the linear system (2.4) is

$$W = \sum_{m,n\in N} \mathbf{f}_{mn} e^{\rho(k_{mn}^2)t} \cos\frac{m\pi x}{l_x} \cos\frac{n\pi y}{l_y}, \tag{2.13}$$

where, see Eqs. (2.2) and (2.7), $k_{mn}^2 = \lambda_{mn}$, and $\mathbf{f}_{mn}$ are the Fourier coefficients determined by the initial data, and $\rho(k_{mn}^2)$ are computed by Eq. (2.8). According to (P_3) in Proposition 2.1, by the expansion (2.13), whether spatial patterns can occur depends on the existence of mode pairs (m, n) satisfying

$$k^2 \equiv \xi^2 + \zeta^2 \in (k_1^2, k_2^2), \quad \text{with} \quad \rho(k^2) > 0, \tag{2.14}$$

where $\xi \equiv m\pi/l_x$ and $\zeta \equiv n\pi/l_y$. In what follows, we assume that, under the zero Neumann boundary conditions and the given domain, there is a unique unstable and admissible mode k satisfying (2.14). We shall denote this mode with k_a and the corresponding chemotactic coefficient with χ_a which is, naturally, larger than χ_c. In a two-dimensional spatial domain, there may be one, two or more mode pairs (m, n) such that

$$k_a^2 \equiv \xi^2 + \zeta^2 = \left(\frac{m\pi}{l_x}\right)^2 + \left(\frac{n\pi}{l_y}\right)^2. \tag{2.15}$$

Accordingly, the eigenvalue λ will be single, double or of higher multiplicity which leads to different types of linear patterns.

3. Stationary patterns

In this section, we apply weakly nonlinear analysis and Fredholm theory to derive amplitude equations for the stationary patterns arising near the critical bifurcation value. We also validate the analytical results by comparing these patterns to the corresponding ones obtained from direct numerical integration and fixed-point iterations of the full system (1.1).

3.1. Weakly nonlinear analysis

We restrict the analysis to the case where patterns are modulated in time but not in space, and note that the evolution of pattern amplitudes is slow near the threshold. Thus, we introduce slow temporal multiple scales as follows:

$$t = t(T_1, T_2, T_3, \dots), \quad T_1 = \varepsilon t, \quad T_2 = \varepsilon^2 t, \quad T_3 = \varepsilon^3 t, \quad \dots, \tag{3.1}$$

where ε is a small parameter accounting for the distance of the system from the bifurcation value χ_a, i.e.

$$\chi = \chi_a + \varepsilon\chi_1 + \varepsilon^2\chi_2 + \varepsilon^3\chi_3 + \cdots, \tag{3.2}$$

and the solution of the original system (1.1) is also expanded as series in ε:

$$W = \varepsilon W_1 + \varepsilon^2 W_2 + \varepsilon^3 W_3 + \cdots \tag{3.3}$$

with W defined as in Eq. (2.5) and $W_i = (W_{1i}, W_{2i})^T$, $i = 1, 2, 3, \dots$. Substituting expansions (3.1)–(3.3) into the original system (1.1) and collecting terms from $O(\varepsilon)$ to $O(\varepsilon^5)$, we obtain the following recursive equations for $W_i, i = 1, 2, 3, 4, 5$, respectively

$$O(\varepsilon^1): \ \mathcal{K}(\chi_a)W_1 = \mathbf{0}, \tag{3.4}$$

$$O(\varepsilon^2): \ \mathcal{K}(\chi_a)W_2 = F(W_1), \tag{3.5}$$

$$O(\varepsilon^3): \ \mathcal{K}(\chi_a)W_3 = G(W_1, W_2), \tag{3.6}$$

$$O(\varepsilon^4): \ \mathcal{K}(\chi_a)W_4 = H(W_1, W_2, W_3), \tag{3.7}$$

$$O(\varepsilon^5): \ \mathcal{K}(\chi_a)W_5 = I(W_1, W_2, W_3, W_4), \tag{3.8}$$

where $\mathcal{K}(\chi_a)$ is defined as in Eq. (2.6) with $\chi = \chi_a$ and

$$F = (F_1, F_2)^T, \quad G = (G_1, G_2)^T, \quad H = (H_1, H_2)^T, \quad I = (I_1, I_2)^T,$$

where the expressions for F_i, G_i, H_i, and I_i can be found in Appendix A.1 for $i = 2$—the expressions corresponding to $i = 1$ are rather lengthy polynomials and are thus omitted in this manuscript for brevity. From Eqs. (2.1)–(2.3), the solution to the linear and homogeneous equation (3.4) with zero Neumann boundary conditions is taken as

$$W_1 = \sum_{i=1}^{p} A_i(T_1, T_2)\, \gamma \cos(\xi_i x) \cos(\zeta_i y), \tag{3.9}$$

which is unique up to a constant multiple and this constant can be absorbed into ε in the expansion (3.3). Here, p is the multiplicity of the eigenvalue λ and the A_i's are the slowly varying amplitudes which will be determined later. γ is the kernel of the following operator

$$\mathcal{K}(\chi_a)|_{W_1} = \begin{pmatrix} -d(u_c)k_a^2 - \mu & \chi_a h(u_c)k_a^2 \\ 1 & -k_a^2 - 1 \end{pmatrix}, \tag{3.10}$$

which is explicitly expressed as

$$\gamma = \begin{pmatrix} 1 + k_a^2 \\ 1 \end{pmatrix},$$

and where we defined

$$d(u) \equiv D(1-u)^{-\alpha}, \qquad h(u) \equiv u(1-u)^{\beta}.$$

We now focus on the two cases where the multiplicity is $p = 1$ (simple) or $p = 2$ (double).

3.2. Patterns for simple eigenvalues

For $p = 1$ the solution (3.9) is of the form

$$W_1 = A(T_1, T_2)\, \gamma \cos(\xi_1 x) \cos(\zeta_1 y). \tag{3.11}$$

It is easy to verify that $\mathcal{K}(\chi_a)$ is a Fredholm operator, cf. the Introduction in [19]. Substituting (3.11) into (3.5) and applying Fredholm theory, i.e. Eq. (3.5) is solvable if and only if the vector F is orthogonal to the kernel of the adjoint of the operator (3.10), we need to impose $\chi_1 = 0$ and $T_1 = 0$. Then, we have a simplified expression for F, by which, the solution to Eq. (3.5) is given and substituted into Eq. (3.6). Again, using Fredholm theory, we obtain the following *Stuart-Landau* equation for the amplitude $A(T_2)$

$$\frac{dA}{dT_2} = \tau A - LA^3, \tag{3.12}$$

corresponding to the normal form of a pitchfork bifurcation which will be responsible for the creation of the patterns. The expressions for the coefficients τ and L are given in Eq. (A.7). The detailed derivation of the evolution Eq. (3.12) is presented in Appendix A.1. It is easy to see that the coefficient τ is always positive and the sign of L depends on $\mathbb{G}_1^{(1)}$ (see Appendix A.1). We shall discuss both the supercritical ($L > 0$) and the subcritical ($L < 0$) cases.

3.2.1. The supercritical case

It is easily verified that the equilibrium $\sqrt{\tau/L}$ of Eq. (3.12) attracts all the positive solutions when $\tau > 0$ and $L > 0$, that is,

$$\lim_{T_2 \to +\infty} A(T_2) = \sqrt{\tau/L} \equiv A_\infty.$$

Therefore, based on the above discussion, we have the following conclusion.

Result 3.1. *The system (1.1) possesses the following stationary pattern with the principal wave number $m/2$ in the x-direction and $n/2$ in the y-direction:*

$$W = \varepsilon A_\infty \gamma \cos(\xi_1 x)\cos(\zeta_1 y) + \varepsilon^2 A_\infty^2 \mathbf{B} \begin{pmatrix} 1 \\ \cos(2\xi_1 x) \\ \cos(2\zeta_1 y) \\ \cos(2\xi_1 x)\cos(2\zeta_1 y) \end{pmatrix} + O(\varepsilon^3), \tag{3.13}$$

where $\mathbf{B} = \begin{pmatrix} b_{11} & b_{12} & b_{13} & b_{14} \\ b_{21} & b_{22} & b_{23} & b_{24} \end{pmatrix}$ *is the coefficient matrix defined in Appendix A.1, provided that, for fixed parameters (D, μ, u_c, α, β) and the given domain and the boundary conditions,*

(1) *$\chi > \chi_c$ and the control parameter $\varepsilon^2 = (\chi - \chi_a)/\chi_a$ is small enough to guarantee that there is only one unstable mode k_a satisfying (2.14);*
(2) *There exists only a pair of positive integers (m, n) such that*

$$k_a^2 = \xi_1^2 + \zeta_1^2, \quad \text{where} \quad \xi_1 \equiv \frac{m\pi}{l_x}, \quad \zeta_1 \equiv \frac{n\pi}{l_y}; \tag{3.14}$$

(3) *The coefficient $L > 0$.*

To validate our analytical results, we now compare them to full numerical solutions of the original system (1.1). All numerical results presented hereby correspond to numerically integrating the full system (1.1) by a combination of second order finite differences in space and fourth order Runge-Kutta in time. We typically integrate the initial condition for $t \in [0, 100]$ and depict the final ($t = 100$) state which, for that time interval, is close to convergence to the stationary state. Letting time run longer (i.e., $t > 100$) has no discernible (visual) difference in the obtained patterns as they have effective converged to the steady state—a notable exception is shown in Fig. 1 where we start from a very small perturbation from the steady state and thus the convergence towards the steady state in rather slow ($t > 100,000$). The domain, in the particular case under consideration, is chosen as $(l_x, l_y) = (3\pi, 3\pi)$ and the system parameters are taken such that $k_1^2 = 1.9063$, $k_2^2 = 2.0750$, $\chi_c = 10.2767$, $\chi_a = 10.2768$, $\tau = 0.9263$ and $L = 88.6484$, and, therefore, there is only one unstable mode $k_a^2 = 2$. Obviously, there exists exactly one pair $(m, n) = (3, 3)$ such that condition (3.14) is satisfied and the solution (3.13) is of the form:

$$W = \varepsilon A_\infty \gamma \cos(x)\cos(y) + \varepsilon^2 A_\infty^2 \mathbf{B} \begin{pmatrix} 1 \\ \cos(2x) \\ \cos(2y) \\ \cos(2x)\cos(2y) \end{pmatrix} + O(\varepsilon^3), \tag{3.15}$$

where $A_\infty = 0.1022$, $\gamma = \begin{pmatrix} 3 \\ 1 \end{pmatrix}$, and $\mathbf{B} = \begin{pmatrix} -11.25 & 18.791 & 18.791 & 18.656 \\ -11.25 & 3.7582 & 3.7582 & 2.0729 \end{pmatrix}$.

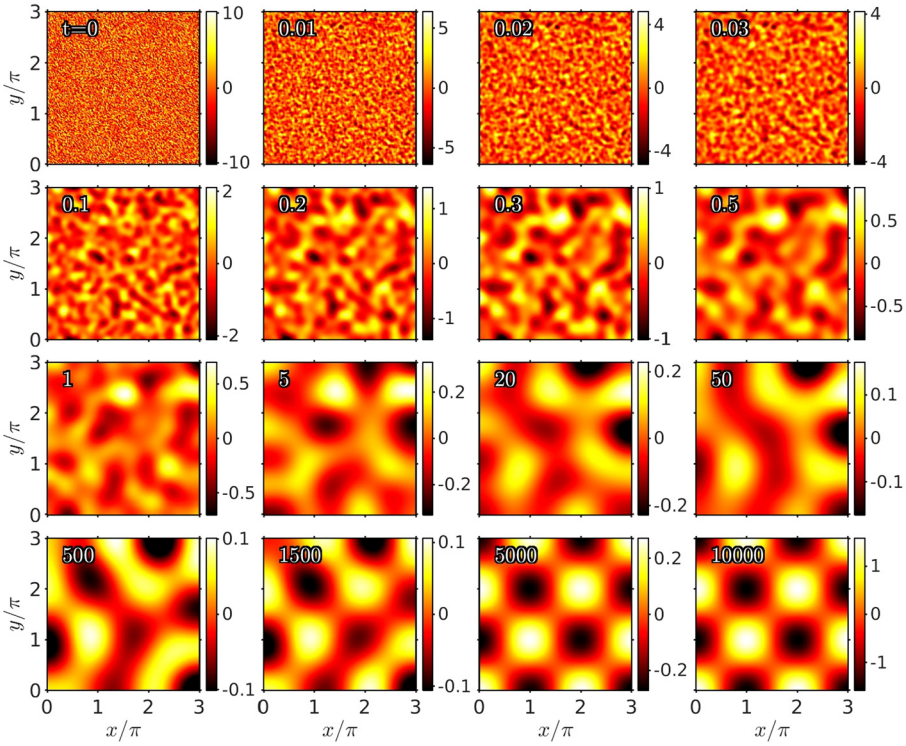

Fig. 1. Evolution of a slightly perturbed homogeneous state in the supercritical case for the system (1.1) with $\varepsilon = 0.02$. Depicted is the perturbation's evolution $(u(x, y, t) - u_c) \times 10^8$ at the times indicated. Parameters are chosen as $D = 0.18$, $\mu = 0.89$, $u_c = 0.2$, $\alpha = 1.0$, $\beta = 0.1$, $\chi = (1 + \varepsilon^2)\chi_a$, and $l_x = l_y = 3\pi$. The initial condition is set as $u_0 = v_0 = u_c + 10^{-7}\sigma(x, y)$ where $\sigma(x, y)$ is a uniform random distribution on the unit square providing a small perturbation about the steady state ω_c. Note that we only show u as the behavior of v is very similar. Also note that the evolution towards the final pattern is slow since ε is relatively small. Larger values of ε lead to similar results albeit a faster convergence to the final pattern (results not shown here).

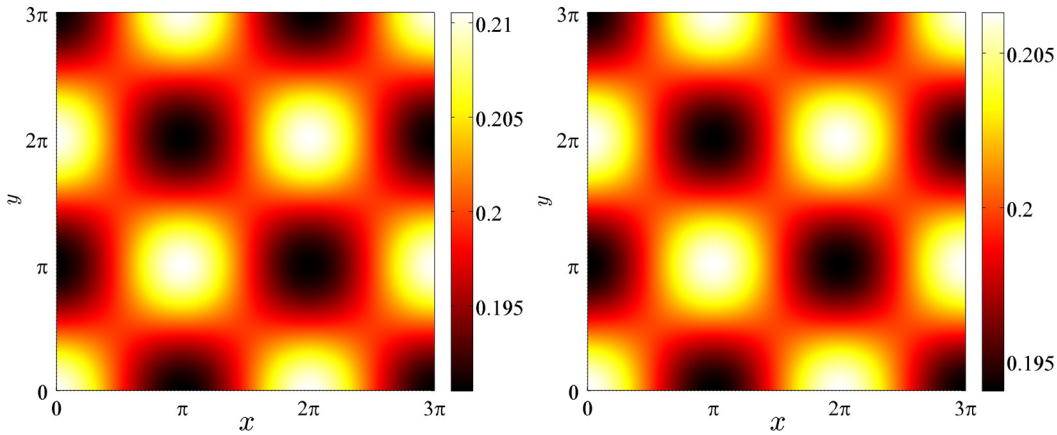

Fig. 2. Steady state for the supercritical case. Patterns for the system (1.1) with the same parameters as in Fig. 1. The initial condition is set as $u_0 = v_0 = u_c + 0.01\sigma(x, y)\cos(3\pi(x - l_x)/l_x)\cos(3\pi(y - l_y)/l_y)$. Left: the numerical solution at $t = 100$ obtained by integrating the full system (1.1). Right: the analytical solution (3.15) obtained by our weakly nonlinear analysis.

Fig. 1 depicts the evolution of the system when starting with a small random initial condition added to the homogeneous state. As it is expected, after an initial period of coarsening, the random initial condition develops localized regions of minima and maxima until the predicted mode ($k_a^2 = 2$) prevails and continues to grow exponentially. If the system is let to evolve further, the configuration will tend towards a steady state that very much resembles the last snapshot shown in Fig. 1 but with a larger amplitude. In what follows, as we are mainly interested in the steady state patterns predicted by a weakly nonlinear analysis,

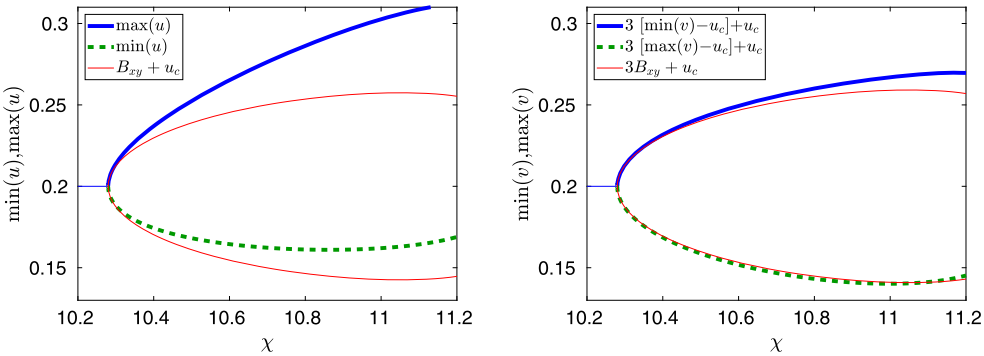

Fig. 3. Bifurcation diagram for the pattern depicted in Fig. 2 as χ is varied. All other parameters are the same as in Fig. 2. The left (right) column corresponds to the u (v) component. The panels depict the minimum and maximum values attained by the patterns. The thick lines correspond to the numerical solutions obtained by fixed-point iterations on the full system (1.1) while the thin lines represent the theoretical approximation given in Eq. (3.15).

we opt to use a more direct (faster) approach for reaching the steady state by giving the initial condition a "head start" along the eigenmode that we are trying to capture. Therefore, we will initialize our system by using an initial condition of the form

$$u_0 = v_0 = u_c + \delta\, \sigma(x, y) f(x, y),$$

where $\sigma(x, y)$ is a uniform, two-dimensional, random distribution on the unit square, δ is the size of the perturbation, and $f(x, y)$ is the eigenmode that we want to capture. Using this initial condition allows for shorter integration times as we are seeding the desired mode from the get-go. Fig. 2 compares the long-time numerical steady state (see left panel) with the prediction (3.15) from our weakly nonlinear analysis (see right panel). As it can be noticed from the figure, there is a very good agreement between the full numerics and the analytical prediction. Note that the agreement is not only on the actual spatial shape of the obtained pattern but, perhaps more importantly, on its final amplitude. In fact, in order to further validate our analytical results, we performed a bifurcation analysis for the steady states of the full system (1.1) as the parameter χ is varied. The steady states of the full system (1.1) were obtained using the nonlinear Newton-Krylov solver `nsoli` [8] and standard continuation (by adiabatically swiping χ) from the solution depicted in Fig. 2 to follow the main bifurcating branches. The results are presented in Fig. 3 by fitting the numerically found steady states for u and v to the ansatz

$$\begin{aligned} w_{\text{ansatz}} = w_c + A_0 + B_{xy}\, \cos(m\pi x/l_x)\, \cos(n\pi y/l_y) + C_x \cos(2m\pi x/l_x) \\ + C_y \cos(2n\pi y/l_y) + C_{xy} \cos(2m\pi x/l_x) \cos(2n\pi y/l_y), \end{aligned} \tag{3.16}$$

where the fitting parameters are A_0, B_{xy}, C_x, C_y, and C_{xy}, and w_c corresponds to u_c or v_c for the respective u and v fittings. As Fig. 3 shows, our weakly nonlinear analysis is able to recover the (pitchfork) bifurcation, from the homogeneous steady state, responsible for the creation of the check-board patterns depicted in Fig. 2.

3.2.2. The subcritical case

If the Landau coefficient $L < 0$, then the equation (3.12) has a unique equilibrium $A = 0$. Obviously, it cannot capture the evolution of the pattern amplitude. We have to push the weakly nonlinear expansion to order $O(\varepsilon^5)$. Then, the following quintic Stuart-Landau equation for the amplitude A is derived:

$$\frac{dA}{dT_2} = \overline{\tau} A - \overline{L} A^3 + \overline{Q} A^5. \tag{3.17}$$

The detailed derivation of Eq. (3.17) is presented in Appendix A.2. Equation (3.17) predicts the bistability of stationary patterns and the possibility of hysteresis cycles for the system (1.1) as some of the parameters of the system (cf. χ) are varied. Further investigation along these lines is presented in Ref. [14]. We now focus on the ensuing stationary patterns. When $\chi > \chi_c$, it is straightforward to verify that $\overline{\tau} > 0$ and $\overline{Q} < 0$, and thus Eq. (3.17) has the unique positive equilibrium

$$\left(\frac{\overline{L} - \sqrt{\overline{L}^2 - 4\overline{Q}\overline{\tau}}}{2\overline{Q}}\right)^{1/2} \equiv A_\infty,$$

where $A_\infty = \lim_{T_2\to\infty} A(T_2)$. We now have the following result:

Result 3.2. *The system (1.1) possesses the steady state pattern with the principal wave number $m/2$ in the x-direction and $n/2$ in the y-direction:*

$$W = \varepsilon A_\infty \gamma \cos(\xi_1 x)\cos(\zeta_1 y) + \varepsilon^2 A_\infty^2 \mathbf{B} \begin{pmatrix} 1 \\ \cos(2\xi_1 x) \\ \cos(2\zeta_1 y) \\ \cos(2\xi_1 x)\cos(2\zeta_1 y) \end{pmatrix} + O(\varepsilon) \tag{3.18}$$

provided that the assumptions (1) and (2) of Result 3.1 are satisfied and

(3) *the Landau coefficient L in Eq. (3.12) is negative.*

Remark 3.1. Notice that $A_\infty = O(\varepsilon^{-1})$ [see Eq. (A.10)], which is different from that in (3.13) and renders (3.18) to be an $O(1)$ perturbation of the equilibrium ω_c.

The numerical example below, see Fig. 4, validates Result 3.2 by comparing it to the solution obtained by directly integrating the full system (1.1). The domain is taken as $l_x = 2\sqrt{2}\pi$, $l_y = 4\pi$, and the system parameters are set to have only one unstable mode $k_a^2 = 1.5$, and $k_1^2 = 1.4240$, $k_2^2 = 1.5450$, $\chi_c = 8.6179$, $\chi_a = 8.6182$, $L = -0.9204$, $\overline{L} = -0.5249$, $\overline{Q} = -17.3218$, and $\overline{\tau} = 0.6751$. There is only the pair $(m, n) = (2, 4)$ such that (3.14) holds. Therefore, the solution (3.18) takes the form:

$$W = \varepsilon A_\infty \gamma \cos(\frac{1}{\sqrt{2}}x)\cos(y) + \varepsilon^2 A_\infty^2 \mathbf{B} \begin{pmatrix} 1 \\ \cos(\sqrt{2}x) \\ \cos(2y) \\ \cos(\sqrt{2}x)\cos(2y) \end{pmatrix} + O(\varepsilon), \tag{3.19}$$

where $A_\infty = 0.4617$, $\gamma = \begin{pmatrix} 2.5 \\ 1 \end{pmatrix}$ and $\mathbf{B} = \begin{pmatrix} -7.8125 & -25.6348 & 9.9712 & 9.4497 \\ -7.8125 & -8.5449 & 1.9942 & 1.3500 \end{pmatrix}$. From Fig. 4, it is seen that the analytical result is in good agreement with the full numerical simulation of system (1.1). The subtle differences originate from omitting higher order terms in the analysis.

3.3. Patterns for double eigenvalues

In this section, we study the pattern formation for the case where $p = 2$ in Eq. (3.9). Hence, the solution $W_1 = (W_{11}, W_{21})$ of Eq. (3.4) has the following form

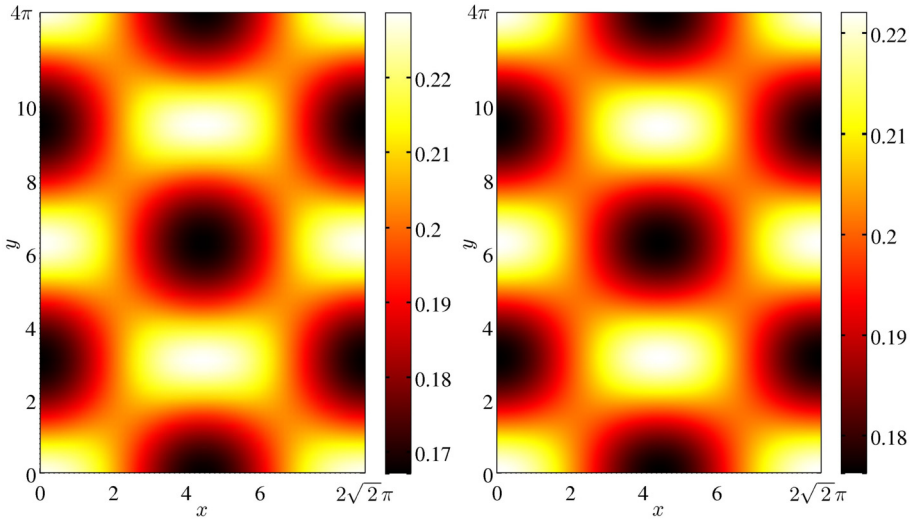

Fig. 4. Subcritical case. Same as in Fig. 2 with parameters $D = 0.2$, $\mu = 0.55$, $u_c = 0.2$, $\alpha = 1.0$, $\beta = 0.5$, $\chi = (1+\varepsilon^2)\chi_a$, $l_x = 2\sqrt{2}\pi$, $l_y = 4\pi$, and the initial condition $u_0 = v_0 = u_c + 0.01\sigma(x,y)\cos(2\pi(x-l_x)/l_x)\cos(4\pi(y-l_y)/l_y)$. Left: the simulation solution of the system (1.1) at $t = 100$. Right: the analytical solution (3.19) obtained by the weakly nonlinear analysis.

$$\begin{cases} W_{11} = A_1(1+k_a^2)\cos(\xi_1 x)\cos(\zeta_1 y) + A_2(1+k_a^2)\cos(\xi_2 x)\cos(\zeta_2 y), \\ W_{21} = A_1\cos(\xi_1 x)\cos(\zeta_1 y) + A_2\cos(\xi_2 x)\cos(\zeta_2 y), \end{cases} \tag{3.20}$$

where

$$\xi_i^2 + \zeta_i^2 = k_a^2 \quad \text{with} \quad \xi_i \equiv \frac{m_i\pi}{l_x}, \quad \zeta_i \equiv \frac{n_i\pi}{l_y}, \quad i = 1, 2.$$

To derive the equation governing the evolution of the pattern amplitude, we need to discuss two cases corresponding to non-resonant and resonant conditions.

3.3.1. Patterns for the non-resonant condition

Assume that the following non-resonant condition is satisfied:

$$\xi_i + \xi_j \neq \xi_j \quad \text{or} \quad \zeta_i + \zeta_j \neq \zeta_j \tag{3.21}$$

and

$$\xi_i - \xi_j \neq \xi_j \quad \text{or} \quad \zeta_i - \zeta_j \neq \zeta_j \tag{3.22}$$

with $i, j = 1, 2$ and $i \neq j$ and the supercritical case holds. Again, the weakly nonlinear analysis up to the order $O(\varepsilon^3)$ and the solvability condition for Eqs. (3.5) and (3.6) are used to derive the following two coupled Landau equations for the amplitudes A_1 and A_2:

$$\begin{cases} \dfrac{dA_1}{dT_2} = \tau A_1 - L_1 A_1^3 + \Omega_1 A_1 A_2^2, \\ \dfrac{dA_2}{dT_2} = \tau A_2 - L_2 A_2^3 + \Omega_2 A_2 A_1^2, \end{cases} \tag{3.23}$$

where $\tau > 0$. The derivation of Eq. (3.23) is presented in Appendix B.1. Under the appropriate conditions, the system (3.23) has four non-negative equilibria

Table 1
Conditions for the existence and stability of the four equilibria listed in Eq. (3.24).

	Existence	Stability condition
(i)	always exists	always unstable
(ii)	$L_1 > 0$	$L_1 + \Omega_2 < 0$
(iii)	$L_2 > 0$	$L_2 + \Omega_1 < 0$
(iv)	$L_1L_2 - \Omega_1\Omega_2 < 0$ $L_2 + \Omega_1 < 0$ $L_1 + \Omega_2 < 0$	always unstable
or		
	$L_1L_2 - \Omega_1\Omega_2 > 0$ $L_2 + \Omega_1 > 0$ $L_1 + \Omega_2 > 0$	$2L_1L_2 + L_1\Omega_1 + L_2\Omega_2 > 0$

$$(i)\ \Big(0,0\Big),\ (ii)\ \Big(\sqrt{\tfrac{\tau}{L_1}},0\Big),\ (iii)\ \Big(0,\sqrt{\tfrac{\tau}{L_2}}\Big),\ (iv)\ \Big(\sqrt{\tfrac{L_2\tau+\Omega_1\tau}{L_1L_2-\Omega_1\Omega_2}},\sqrt{\tfrac{L_1\tau+\Omega_2\tau}{L_1L_2-\Omega_1\Omega_2}}\Big), \tag{3.24}$$

where the first coordinate denotes the amplitude A_1 and the second one denotes A_2. The conditions for the existence and linear stability of the four equilibria are listed in the Table 1.

We now state the result on the non-resonant supercritical case.

Result 3.3. *If the following assumptions are satisfied*

(1) *The parameters D, μ, u_c, α and β are fixed, and $\chi > \chi_c$. For the given domain and the boundary conditions, the control parameter $\varepsilon^2 = (\chi - \chi_a)/\chi_a$ is small enough to guarantee that there is only a single unstable mode k_a satisfying (2.14);*
(2) *There exist two pairs of positive integers $(m_i, n_i), i = 1, 2$ such that*

$$k_a^2 = \xi_i^2 + \zeta_i^2 \quad \text{with} \quad \xi_i \equiv \frac{m_i\pi}{l_x}, \quad \zeta_i \equiv \frac{n_i\pi}{l_y}; \tag{3.25}$$

(3) *The system (3.23) possesses at least one stable positive equilibrium;*

then the stationary pattern for (1.1) has the following explicit expression

$$\begin{aligned} W = {} & \varepsilon\gamma[A_{1\infty}\cos(\xi_1 x)\cos(\zeta_1 y) + A_{2\infty}\cos(\xi_2 x)\cos(\zeta_2 y)] \\ & + \varepsilon^2\left[\left(A_{1\infty}^2 + A_{2\infty}^2\right)\mathbf{B_1}\Upsilon_1 + A_{1\infty}A_{2\infty}\mathbf{B_2}\Upsilon_2\right] + O(\varepsilon^3), \end{aligned} \tag{3.26}$$

where

$$\mathbf{B_1} = \begin{pmatrix} b_{11}^{(1)} & b_{11}^{(2)} & b_{12}^{(1)} & b_{12}^{(2)} & b_{13}^{(1)} & b_{13}^{(2)} & b_{14}^{(1)} & b_{14}^{(2)} \\ b_{21}^{(1)} & b_{21}^{(2)} & b_{22}^{(1)} & b_{22}^{(2)} & b_{23}^{(1)} & b_{23}^{(2)} & b_{24}^{(1)} & b_{24}^{(2)} \end{pmatrix}; \qquad \mathbf{B_2} = \begin{pmatrix} b_{15} & b_{16} & b_{17} & b_{18} \\ b_{25} & b_{26} & b_{27} & b_{28} \end{pmatrix};$$

$$\Upsilon_1 = \begin{pmatrix} 1 \\ 1 \\ \cos(2\xi_1 x) \\ \cos(2\xi_2 x) \\ \cos(2\zeta_1 y) \\ \cos(2\zeta_2 y) \\ \cos(2\xi_1 x)\cos(2\zeta_1 y) \\ \cos(2\xi_2 x)\cos(2\zeta_2 y) \end{pmatrix}; \quad \Upsilon_2 = \begin{pmatrix} \cos(\xi_1+\xi_2)x\cos(\zeta_1+\zeta_2)y \\ \cos(\xi_1+\xi_2)x\cos(\zeta_1-\zeta_2)y \\ \cos(\xi_1-\xi_2)x\cos(\zeta_1+\zeta_2)y \\ \cos(\xi_1-\xi_2)x\cos(\zeta_1-\zeta_2)y \end{pmatrix}$$

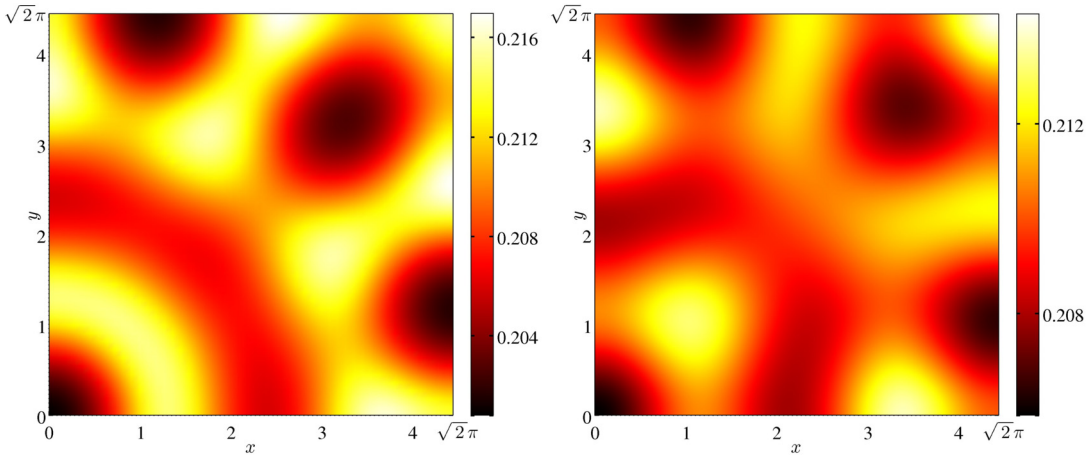

Fig. 5. Case (I) for the non-resonant condition. Shown are the patterns given by Eq. (3.27) (right) and the corresponding numerical solution of Eq. (1.1) (left) with $\varepsilon = 0.015$ at $t = 100$. The system parameters are chosen as $D = 0.1$, $u_c = 0.21$, $\mu = 11.6$, $\alpha = 2.0$, $\beta = -0.8$, $\chi = (1+\varepsilon^2)\chi_a$, and $l_x = l_y = \sqrt{2}\pi$. The initial data is $u_0 = v_0 = u_c + 0.01\sigma(x,y)[\cos(4\pi(x-l_x)/l_x)\cos(\pi(y-l_y)/l_y) + \cos(\pi(x-l_x)/l_x)\cos(4\pi(y-l_y)/l_y)]$.

and $(A_{1\infty}, A_{2\infty})$ is a stable equilibrium point of the system (3.23) which is one of the three positive equilibria (3.24). Which of the three equilibria is chosen by the dynamics depends on the conditions expressed in Table 1 and the initial data. If the equilibria (ii) or (iii) are stable, then single mode patterns will ensue; while mixed mode patterns will emerge when the equilibrium (iv) is stable.

The three mixed mode patterns cases, (I)–(III), are described in detail in Appendix B.1. In the following numerical examples we test the above theoretical results. Figs. 5–7 show, for the three cases (I)–(III), respectively, comparisons between the results obtained from the weakly nonlinear analysis alongside the corresponding ones by solving numerically the full system (1.1).

Fig. 5 depicts the case (I) with the square domain $l_x = l_y = \sqrt{2}\pi$. The chosen parameters lead to the unique unstable mode $k_a^2 = 8.5$ with the mode pairs $(m_1, n_1) = (4, 1)$ and $(m_2, n_2) = (1, 4)$ satisfying (3.25), and $\chi_a = 57.1292$, $\chi_c = 57.1291$ and only the equilibrium (iv) $(A_1, A_2) = (0.0149, 0.0149)$ is stable. Thus, the expression for this stationary pattern is

$$W = \varepsilon\gamma 0.0149\left[\cos\left(\frac{4}{\sqrt{2}}x\right)\cos\left(\frac{1}{\sqrt{2}}y\right) + \cos\left(\frac{1}{\sqrt{2}}x\right)\cos\left(\frac{4}{\sqrt{2}}y\right)\right] + \varepsilon^2 0.0149^2\left(2\mathbf{B_1}\Upsilon_1 + \mathbf{B_2}\Upsilon_2\right)|_{(\mathrm{I})} + O(\varepsilon^3). \tag{3.27}$$

In Fig. 5 we see that the theoretical and numerical solutions are qualitatively similar. However, a significant quantitative discrepancy can be seen. We believe that this discrepancy is due to the appearance of the subharmonic $(m, n) = (3, 3)$ which has the same order of magnitude as the modes $(m, n) = (4, 1)$ and $(m, n) = (1, 4)$. It is easy to check that the subharmonic $(m, n) = (3, 3)$ corresponds to the discrete eigenvalue $k^2 = 9$ which is close to $k_a^2 = 8.5$ and makes the lower order damping mechanism unable to overcome the higher order excitation mechanism coming from the interaction of the main harmonics $(m, n) = (4, 1)$ and $(m, n) = (1, 4)$.

Fig. 6 depicts case (II) for the rectangular domain $(l_x, l_y) = (\sqrt{2}\pi, \pi)$ and parameter values chosen in such a way that only the mode $k_a^2 = 9$ is allowed. In this case, $\chi_a = 63.2002$, $\chi_c = 63.2000$, and the uniform steady state is linearly unstable to the two mode pairs $(m_1, n_1) = (0, 3)$ and $(m_2, n_2) = (4, 1)$. Furthermore, only the mixed mode steady state (iv) $(A_1, A_2) = (0.0164, 0.0299)$ is stable. Therefore, the predicted solution is

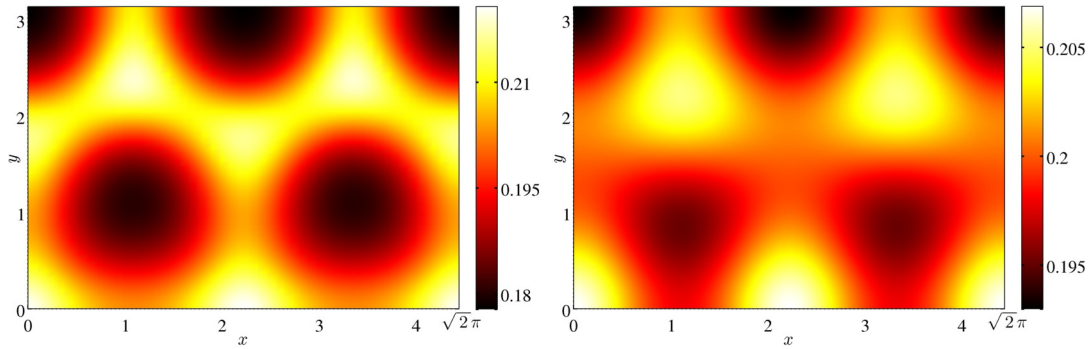

Fig. 6. Case (II) for the non-resonant condition. Patterns given by Eq. (3.28) (right) and the corresponding numerical solution of the full system (1.1) (left) with $\varepsilon = 0.015$ are depicted at $t = 100$. The system parameters are $D = 0.1$, $u_c = 0.2$, $\mu = 10$, $\alpha = 1.0$, $\beta = 0.1$, $\chi = (1 + \varepsilon^2)\chi_a$, and $l_x = \sqrt{2}\pi$, $l_y = \pi$. The initial data are $u_0 = v_0 = u_c + 0.01\sigma(x, y)[\cos(3\pi(y - l_y)/l_y) + \cos(4\pi(x - l_x)/l_x)\cos(\pi(y - l_y)/l_y)]$.

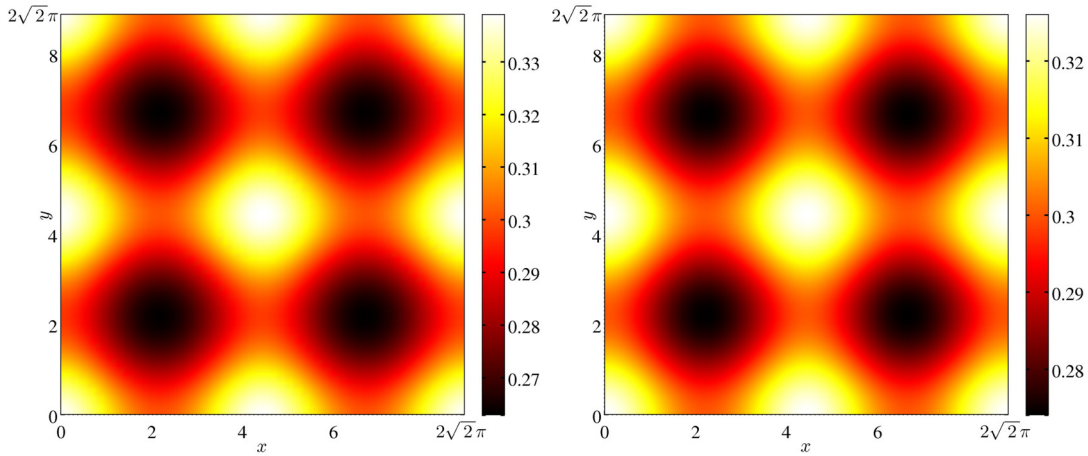

Fig. 7. Case (III) for the non-resonant condition. Patterns given by Eq. (3.29) (right) and the corresponding numerical solution of the full system (1.1) (left) with $\varepsilon = 0.04$ are depicted at $t = 100$. The system parameters are taken as $D = 0.16$, $u_c = 0.3$, $\mu = 0.9$, $\alpha = 0.8$, $\beta = 0.4$, $\chi = (1 + \varepsilon^2)\chi_a$, and $l_x = l_y = 2\sqrt{2}\pi$. The initial data is $u_0 = v_0 = u_c + 0.01\sigma(x, y)[\cos(4\pi(y - l_y)/l_y) + \cos(4\pi(x - l_x)/l_x))]$.

$$W = \varepsilon\gamma\left[0.0164\cos(3y) + 0.0299\cos\left(\frac{4}{\sqrt{2}}x\right)\cos y\right] \tag{3.28}$$
$$+ \varepsilon^2\left[\left(0.0164^2 + 0.0299^2\right)\mathbf{B_1}\Upsilon_1 + 0.0164 \times 0.0299\mathbf{B_2}\Upsilon_2\right]|_{(\mathrm{II})} + O(\varepsilon^3).$$

In Fig. 6 it is seen that the expected solution (3.28) can qualitatively, and to some extent quantitatively, describe the stationary patterns. Nonetheless, there is a subtle quantitative discrepancy which results, similar to the previous case, from the presence of the harmonics $(m, n) = (3, 2)$ and $(m, n) = (1, 3)$ corresponding to $k^2 = 8.5$ and $k^2 = 9.5$ which are close to $k_a^2 = 9$.

Fig. 7 depicts an example for case (III) with the square domain $l_x = l_y = 2\sqrt{2}\pi$. In this case, the system parameters yield the unique unstable mode $k_a^2 = 2$ with the following mode pairs satisfying Eq. (3.25): $(m_1, n_1) = (0, 4)$ and $(m_2, n_2) = (4, 0)$ with $\chi_a = 7.6448$ and $\chi_c = 7.6435$. Therefore, the only stable mixed mode steady state is (iv) $(A_1, A_2) = (0.1019, 0.1019)$ and, thus, the asymptotic expression of the emerging solution to second order is:

$$W = \varepsilon\gamma 0.1019\left(\cos(\sqrt{2}y) + \cos(\sqrt{2}x)\right) + \varepsilon^2 0.1019^2\left(2\mathbf{B_1}\Upsilon_1 + \mathbf{B_2}\Upsilon_2\right)|_{(\mathrm{III})} + O(\varepsilon^3). \tag{3.29}$$

In Fig. 7 it is shown that the solution predicted by the weakly nonlinear analysis is in excellent agreement with the numerical simulation of the original system.

3.3.2. Patterns for the resonant condition

We now discuss the case where the resonant condition holds, that is,

$$\xi_i + \xi_j = \xi_j \quad \text{and} \quad \zeta_i - \zeta_j = \zeta_j \tag{3.30}$$

or

$$\xi_i - \xi_j = \xi_j \quad \text{and} \quad \zeta_i + \zeta_j = \zeta_j$$

with $i, j = 1, 2$ and $i \neq j$. In the following discussion, we assume that, without loss of generality, the first condition (3.30) is satisfied with $i = 1$ and $j = 2$ and, thus, we have the following relations:

$$\xi_1 = 0, \quad \xi_2 = \sqrt{3}\zeta_2 = \frac{\sqrt{3}}{2}k_a, \quad \zeta_1 = 2\zeta_2 = k_a, \quad \text{and} \quad l_y = \frac{n_2}{m_2}\sqrt{3}l_x. \tag{3.31}$$

We can now rewrite the solution (3.9) of the system (3.4) as

$$W_1 = A_1(T_1, T_2)\gamma\cos(2\zeta_2 y) + A_2(T_1, T_2)\gamma\cos(\sqrt{3}\zeta_2 x)\cos(\zeta_2 y). \tag{3.32}$$

The solvability condition for Eq. (3.5) results in the following system for the amplitudes A_1 and A_2

$$\begin{cases} \dfrac{\partial A_1}{\partial T_1} = \tau A_1 - \dfrac{L}{4}A_2^2, \\ \dfrac{\partial A_2}{\partial T_1} = \tau A_2 - LA_1A_2. \end{cases} \tag{3.33}$$

The derivation of this system is presented in Appendix B.2. Obviously, the equilibria $(0, 0)$ and $(\tau/L, \pm 2\tau/L)$ of Eq. (3.33) are all unstable whether L is positive or negative. Thus the asymptotic analysis has to be pushed to higher order to obtain the amplitude equations for A_1 and A_2. Therefore, up the order $O(\varepsilon^3)$ the Stuart-Landau's yield:

$$\begin{cases} \dfrac{dA_1}{dt} &= \bar{\tau}_1 A_1 - \bar{L}_1 A_2^2 + \bar{\Omega}_1 A_1 A_2^2 + \bar{\Psi}_1 A_1^3, \\ \dfrac{dA_2}{dt} &= \bar{\tau}_2 A_2 - \bar{L}_2 A_1 A_2 + \bar{\Omega}_2 A_1^2 A_2 + \bar{\Psi}_2 A_2^3, \end{cases} \tag{3.34}$$

where the expressions of the coefficients are presented in Appendix B.2. We now give the main result of the weakly nonlinear analysis for the resonant case:

Result 3.4. *The stationary pattern for (1.1) has the following explicit expression*

$$W = \varepsilon\gamma(A_{1\infty}\cos(2\zeta_2 y) + A_{2\infty}\cos(\sqrt{3}\zeta_2 x)\cos(\zeta_2 y)) + \varepsilon^2\overline{\Upsilon} + O(\varepsilon^3), \tag{3.35}$$

where $\overline{\Upsilon}$ is W_2 defined as (B.4), provided that

(1) *The parameters D, μ, u_c, α and β are fixed, and $\chi > \chi_c$. For the given domain and the boundary conditions the control parameter $\varepsilon^2 = (\chi - \chi_a)/\chi_a$ is small enough so that the uniform steady state (u_c, u_c) is unstable to two modes corresponding only to the eigenvalue k_a;*

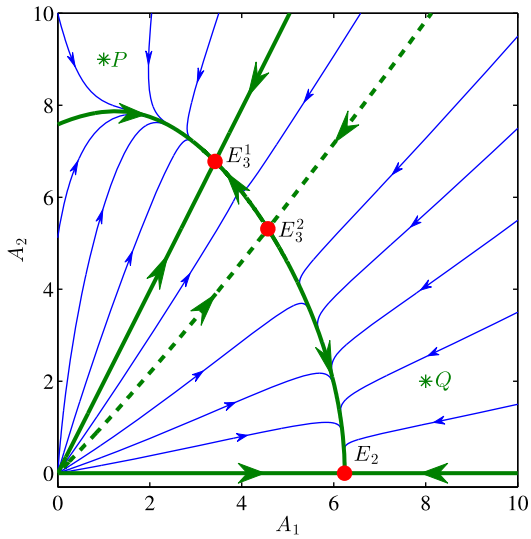

Fig. 8. Typical phase portrait of system (3.34). The values for the parameters are: $D = 6.0$, $u_c = 0.3$, $\mu = 1.7$, $\alpha = 1.0$ and $\beta = 0.14$. The non-negative steady states $E_2 = (6.2350, 0)$ and $E_3^1 = (3.3998, 6.7998)$ are stable nodes while $E_3^2 = (4.5877, 5.2799)$ is a saddle point with eigenvectors $(0.6225, 0.7826)^T$ and $(-0.5322, 0.8466)^T$. The manifolds emanating from the fixed points are depicted by thick (green) solid and dashed lines. The dashed line depicts the stable manifolds of E_3^2 that correspond to the separatrix between the two different dynamical outcomes presented in Figs. 9 and 10. (For interpretation of the colors in the figure(s), the reader is referred to the web version of this article.)

(2) *There exist two pairs of positive integers* $(m_i, n_i), i = 1, 2$ *such that*

$$k_a^2 = \xi_i^2 + \zeta_i^2 \quad \text{with} \quad \xi_i = \frac{m_i \pi}{l_x}, \quad \zeta_i = \frac{n_i \pi}{l_y}; \tag{3.36}$$

(3) ξ_i *and* ζ_i *satisfy the resonant condition (3.30) and* $(A_{1\infty}, A_{2\infty})$ *is a stable non-negative steady state of the system (3.34).*

The non-negative steady states of the system (3.34) has three types. The trivial case where $E_1 = (0, 0)$ is always unstable, the semi-trivial case is $E_2 = (\sqrt{-\bar{\tau}_1/\bar{\Psi}_1}, 0)$, and the non-trivial case where $E_3 = (A_1, A_2)$ with both A_1 and A_2 not equal to zero and satisfying the following system

$$\begin{cases} (\bar{\Psi}_1\bar{\Psi}_2 - \bar{\Omega}_1\bar{\Omega}_2)A_1^3 + (\bar{\Omega}_1\bar{L}_2 + \bar{\Omega}_2\bar{L}_1)A_1^2 + (\bar{\tau}_1\bar{\Psi}_2 - \bar{L}_1\bar{L}_2 - \bar{\Omega}_1\bar{\tau}_2)A_1 + \bar{\tau}_2\bar{L}_1 = 0, \\ A_2^2 = \frac{1}{\bar{\Psi}_2}(\bar{L}_2 A_1 - \bar{\Omega}_2 A_1^2 - \bar{\tau}_2). \end{cases} \tag{3.37}$$

Due to the complicated expressions for all the coefficients in Eqs. (3.34) and (3.37), it is not possible to explicitly determine the stability conditions for the last two types. Therefore, we use a numerical example displaying a typical scenario.

The example in Fig. 8 depicts the phase portrait for the system (3.34) for the rectangular domain where $(l_x, l_y) = (\sqrt{3}\pi, 9\pi)$ with $\chi_c = 62.7425$, $\chi_a = 62.7426$ and the unique unstable discrete mode $k_a^2 = \frac{4}{9}$ satisfying (3.36). Accordingly, the uniform steady state is linearly unstable to the two mode pairs $(m_1, n_1) = (0, 6)$ and $(m_2, n_2) = (1, 3)$. As Fig. 8 indicates, through the existence of a separatrix (see dashed line), the shape of the stationary pattern depends on the initial values of A_1 and A_2 [namely, on which side of the separatrix the initial (A_1, A_2) is].

Figs. 9 and 10 correspond, respectively, to the initial values $(A_1, A_2) = (1, 9)$ and $(A_1, A_2) = (8, 2)$ (see, respectively, points P and Q in Fig. 8). P and Q lie, respectively, on the attractive basins for E_3^1 and E_2 (see Fig. 8). Thus the asymptotic pattern starting from P is hexagonal and it is predicted by the following solution

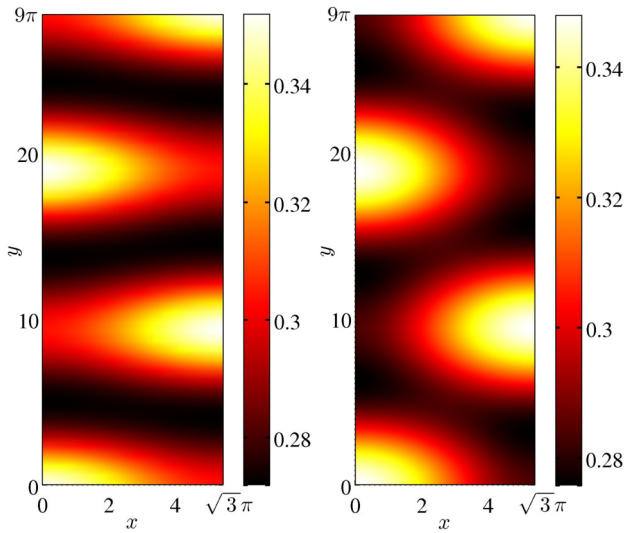

Fig. 9. Resonant case with $(A_1, A_2) = (1, 9)$. Shown are the prediction from Eq. (3.38) (right) and the corresponding numerical simulation of the full system (1.1) (left) at $t = 100$ for $\varepsilon = 0.004$. Same parameter values as in Fig. 8 with $\chi = (1 + \varepsilon + \varepsilon^2)\chi_a$ and $l_x = \sqrt{3}\pi$, $l_y = 9\pi$. The initial data are set as $u_0 = v_0 = u_c + 0.01\sigma(x, y)[\cos(6\pi(y - l_y)/l_y) + 9\cos(\pi(x - l_x)/l_x)\cos(3\pi(y - l_y)/l_y)]$. The initial condition corresponds to the point P depicted in the phase portrait diagram in Fig. 8.

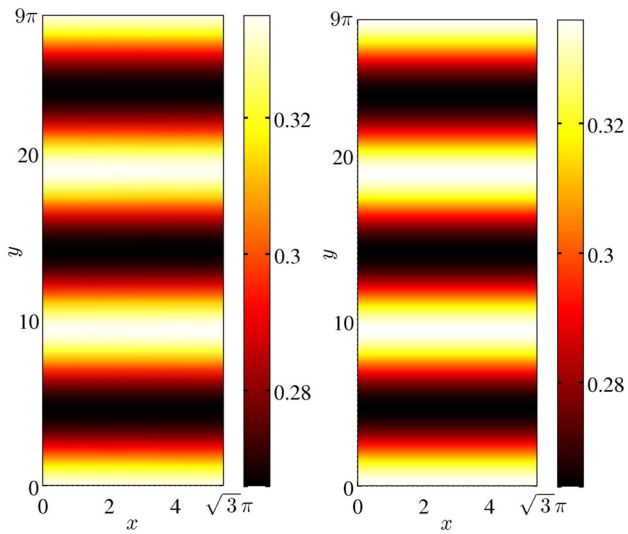

Fig. 10. Same as in Fig. 9 for the resonant case with $(A_1, A_2) = (8, 2)$. The initial condition is, in this case, $u_0 = v_0 = u_c + 0.01\sigma(x, y)[8\cos(6\pi(y - l_y)/l_y) + 2\cos(\pi(x - l_x)/l_x)\cos(3\pi(y - l_y)/l_y)]$. The initial condition corresponds to the point Q depicted in the phase portrait diagram in Fig. 8.

$$W = \varepsilon\gamma\left[3.3998\cos\left(\frac{2}{3}y\right) + 6.7998\cos\left(\frac{\sqrt{3}}{3}x\right)\cos\left(\frac{1}{3}y\right)\right] + \varepsilon^2\overline{\Upsilon}|_{E_3^1} + O(\varepsilon^3), \tag{3.38}$$

while the asymptotic pattern when starting at the point Q is a rolling one and has the form:

$$W = 6.2350\varepsilon\gamma\cos\left(\frac{2}{3}y\right) + \varepsilon^2\overline{\Upsilon}|_{E_2} + O(\varepsilon^3). \tag{3.39}$$

From Figs. 9 and 10 it follows that the expression (3.35) obtained by the weakly nonlinear analysis captures nicely the asymptotic stationary pattern of the system (1.1).

4. Conclusions

In this paper we study the emergence and dynamics of patterns in a two-dimensional, rectangular, domain for a chemotaxis model with nonlinear diffusion and volume-filling effect. Using a weakly nonlinear multiple scales analysis, we derive the amplitude equations and establish the asymptotic formulae for stationary patterns for both the single eigenvalue case including supercritical and subcritical phenomena and the double eigenvalue case including resonant and non-resonant eigenvalues. We employ this weakly nonlinear methodology to obtain a wide diversity of stationary patterns supported by the system. In particular, we put forward asymptotic expressions for mixed-mode, square, hexagonal, and roll stationary configurations. We find these analytical predictions to be in very good agreement with full numerical simulations of the original system.

As possible avenues for future research, a similar analysis as the one presented here for rectangular domains could be developed for more general domains involving their respective eigenfunctions. It would also be interesting to further study the chemotaxis system by analyzing the hysteresis phenomenon induced by the existence of a supercritical pitchfork bifurcation for appropriate parameters ranges. Some innovative results could be obtained by applying the global bifurcation theory recently developed in [19] to the model (1.1). On the other hand, motivated by the research in [17,23] where authors suggested that the cellular growth leads to the emergence of time-periodic patterns, it would be intriguing to establish the existence of time-periodic patterns appearing in (1.1). Finally, it would also be relevant to study the cross-roll instability corresponding to the resonant case. These topics are currently under investigation and will be reported in a future publication.

Acknowledgments

The work of M. Ma is supported by National Natural Science Foundation of China (No. 11671359, No. 11271342), provincial Natural Science Foundation of Zhejiang (No. LY19A010027, No. LY18A010013) and Science Foundation of Zhejiang Sci-Tech University under Grant (No. 15062173-Y). R.C.G. acknowledges support from NSF-PHY-1603058.

Appendix A. Stuart-Landau equation for simple eigenvalue

This appendix gives the detailed derivation of the amplitude equation for $p = 1$.

A.1. The cubic Stuart-Landau equation

In Eqs. (3.5)–(3.8), the expressions of non-homogeneous terms are as follows:

$$\begin{cases} F_1 = \dfrac{\partial W_{11}}{\partial T_1} + \dfrac{\mu}{u_c} W_{11}^2 - d'(u_c)\nabla\cdot(W_{11}\nabla W_{11}) + \chi_m h'(u_c)\nabla\cdot(W_{11}\nabla W_{21}) + \chi_1 h(u_c)\Delta W_{21}, \\ F_2 = \dfrac{\partial W_{21}}{\partial T_1}, \end{cases} \tag{A.1}$$

$$G_2 = \frac{\partial W_{22}}{\partial T_1} + \frac{\partial W_{21}}{\partial T_2},\ H_2 = \frac{\partial W_{21}}{\partial T_3} + \frac{\partial W_{22}}{\partial T_2} + \frac{\partial W_{23}}{\partial T_1},\ I_2 = \frac{\partial W_{21}}{\partial T_4} + \frac{\partial W_{22}}{\partial T_3} + \frac{\partial W_{23}}{\partial T_2} + \frac{\partial W_{24}}{\partial T_1}, \tag{A.2}$$

and the explicit expressions of G_1, H_1 and I_1 are omitted here for brevity. In the considered case, the solution for Eq. (3.4) is given by

$$W_1 = A(T_1, T_2)\gamma\cos(\xi_1 x)\cos(\zeta_1 y). \tag{A.3}$$

Substituting this into Eq. (3.5) yields

$$F_1 = \left[\frac{\partial A}{\partial T_1}(1+k_a^2) - A\chi_1 h(u_c)k_a^2\right]\cos(\xi_1 x)\cos(\zeta_1 y) + A^2\sum_{i,j}\Gamma_{w_{ij}}\cos(i\xi_1 x)\cos(j\zeta_1 y),$$

$$F_2 = \frac{\partial A_1}{\partial T_1}\cos(\xi_1 x)\cos(\zeta_1 y)$$

with $i = 0, 2$, $j = 0, 2$; $\omega_{00} = 0$, $\omega_{20} = \xi_1$, $\omega_{02} = \zeta_1$, $\omega_{22} = k_a$, and

$$\Gamma_{w_{ij}} = \frac{\mu}{4u_c}(1+k_a^2)^2 + \frac{1}{2}d'(u_c)(1+k_a^2)^2\omega_{ij}^2 - \frac{1}{2}\chi_m h'(u_c)(1+k_a^2)\omega_{ij}^2.$$

By a simple computation, the solution of the adjoint system of (3.4) is

$$\overline{W}_1 = A(T_1, T_2)\overline{\gamma}\cos(\xi_1 x)\cos(\zeta_1 y), \quad \overline{\gamma} = \begin{pmatrix} 1+k_a^2 \\ \chi_a h(u_c)k_a^2 \end{pmatrix}, \tag{A.4}$$

where $\overline{\gamma}$ is the kernel of the adjoint operator of (3.10). In order to satisfy the solvability condition for Eq. (3.5), i.e. $\langle F, \overline{W}_1\rangle = 0$, where $\langle\cdot,\cdot\rangle$ is the scalar product in $[0, l_x]\times[0, l_y]$, we need let $\chi_1 = 0$ and $T_1 = 0$. Then, the solution to Eq. (3.5) can be given by

$$W_2 = A^2\begin{pmatrix} b_{11} & b_{12} & b_{13} & b_{14} \\ b_{21} & b_{22} & b_{23} & b_{24} \end{pmatrix}\begin{pmatrix} 1 \\ \cos(2\xi_1 x) \\ \cos(2\zeta_1 y) \\ \cos(2\xi_1 x)\cos(2\zeta_1 y) \end{pmatrix}. \tag{A.5}$$

Plugging this solution into Eq. (3.6) and using the method of undetermined coefficient, we obtain that the coefficients b_{ij} $(i = 1, 2; j = 1, 2, 3, 4)$ satisfy:

$$\kappa_{ij}(\chi_a)\begin{pmatrix} b_{1p} \\ b_{2p} \end{pmatrix} = \begin{pmatrix} \Gamma_{\omega_{ij}} \\ 0 \end{pmatrix},$$

where

$$\omega_{00} = 0 \text{ with } p = 1,\ \omega_{20} = \xi_1 \text{ with } p = 2,\ \omega_{02} = \zeta_1 \text{ with } p = 3,\ \omega_{22} = k_a \text{ with } p = 4$$

and

$$\kappa_{ij}(\chi_a) = \begin{pmatrix} -d(u_c)(i^2\xi_1^2 + j^2\zeta_1^2) - \mu & \chi_m h(u_c)(i^2\xi_1^2 + j^2\zeta_1^2) \\ 1 & -(i^2\xi_1^2 + j^2\zeta_1^2) - 1 \end{pmatrix}. \tag{A.6}$$

We now substitute W_2 into Eq. (3.6), then $G = (G_1, G_2)^T$ can be written as

$$G = \left[\frac{dA}{dT_2}\gamma - \mathbb{G}_1^{(0)}A + \mathbb{G}_1^{(1)}A^3\right]\cos(\xi_1 x)\cos(\zeta_1 y)$$
$$+ \left[\mathbb{G}_1^{(2)}\cos(3\xi_1 x)\cos(\zeta_1 y) + \mathbb{G}_1^{(3)}\cos(\xi_1 x)\cos(3\zeta_1 y) + \mathbb{G}_1^{(4)}\cos(3\xi_1 x)\cos(3\zeta_1 y)\right]A^3,$$

where $\mathbb{G}_1^{(i)} = \begin{pmatrix} G_1^{(i)} \\ 0 \end{pmatrix}$, with $G_1^{(0)} = \chi_2 h(u_c)k_a^2$ and $G_1^{(i)}, i = 1, 2, 3, 4$ are lengthy polynomials and omitted here. Again, using the solvability condition for Eq. (3.6), we have $\langle G, \overline{W}_1 \rangle = 0$ which leads to the cubic Stuart-Landau equation (3.12) for the amplitude $A(T_2)$, where the expressions for the coefficients τ and L are:

$$\tau = \frac{\langle \mathbb{G}_1^{(0)}, \overline{\gamma} \rangle}{\langle \gamma, \overline{\gamma} \rangle} = \frac{\chi_2 h(u_c)k_a^2(1+k_a^2)}{(1+k_a^2)^2 + \chi_a h(u_c)k_a^2}, \quad L = \frac{\langle \mathbb{G}_1^{(1)}, \overline{\gamma} \rangle}{\langle \gamma, \overline{\gamma} \rangle} = \frac{(1+k_a^2)G_1^{(1)}}{(1+k_a^2)^2 + \chi_a h(u_c)k_a^2}. \tag{A.7}$$

A.2. The quintic Stuart-Landau equation

If the Landau coefficient L in Eq. (3.12) is negative, it follows that this equation cannot describe the pattern amplitude for system (1.1). Thus, it is necessary to perform the nonlinear analysis up to order $O(\varepsilon^5)$. For simplicity, in this section we replace ξ_1 and ζ_1 by ϕ and ψ, respectively; furthermore, let $M = 1 + k_a^2$ in the rest of the appendix.

According to the expression of G, the solution to Eq. (3.6) is

$$W_3 = \mathbf{C} \begin{pmatrix} \cos(\phi x)\cos(\psi y) \\ \cos(3\phi x)\cos(\psi y) \\ \cos(\phi x)\cos(3\psi y) \\ \cos(3\phi x)\cos(3\psi y) \end{pmatrix}, \tag{A.8}$$

where $\mathbf{C} = \begin{pmatrix} c_{11}A + c_{12}A^3 & c_{13}A^3 & c_{14}A^3 & c_{15}A^3 \\ c_{21}A + c_{22}A^3 & c_{23}A^3 & c_{24}A^3 & c_{25}A^3 \end{pmatrix}$, and c_{ij} $(i = 1, 2; j = 1, 2, 3, 4)$ satisfy

$$\kappa_{11}(\chi_a)\begin{pmatrix} c_{11} \\ c_{21} \end{pmatrix} = \begin{pmatrix} \tau M - G_1^{(0)} \\ \tau \end{pmatrix}, \quad \kappa_{11}(\chi_a)\begin{pmatrix} c_{12} \\ c_{22} \end{pmatrix} = \begin{pmatrix} G_1^{(1)} - LM \\ -L \end{pmatrix},$$
$$\kappa_{31}(\chi_a)\begin{pmatrix} c_{13} \\ c_{23} \end{pmatrix} = \begin{pmatrix} G_1^{(2)} \\ 0 \end{pmatrix}, \ \kappa_{13}(\chi_a)\begin{pmatrix} c_{14} \\ c_{24} \end{pmatrix} = \begin{pmatrix} G_1^{(3)} \\ 0 \end{pmatrix}, \ \kappa_{33}(\chi_a)\begin{pmatrix} c_{15} \\ c_{25} \end{pmatrix} = \begin{pmatrix} G_1^{(4)} \\ 0 \end{pmatrix}$$

with $\kappa_{ij}(\chi_a)$ defined in Eq. (A.6). Then, plugging W_1, W_2 and W_3 into Eq. (3.7) yields

$$\begin{aligned} H_1 &= \left[H_1^{(1)}A^2 + H_1^{(2)}A^4\right] + \left[H_2^{(1)}A^2 + H_2^{(2)}A^4\right]\cos(2\phi x) + \left[H_3^{(1)}A^2 + H_3^{(2)}A^4\right]\cos(2\psi y) \\ &\quad + \left[H_4^{(1)}A^2 + H_4^{(2)}A^4\right]\cos(2\phi x)\cos(2\psi y) + H_5^{(2)}A^4\cos(4\phi x) + H_6^{(2)}A^4\cos(4\psi y) \\ &\quad + H_7^{(2)}A^4\cos(4\phi x)\cos(2\psi y) + H_8^{(2)}A^4\cos(2\phi x)\cos(4\psi y) + H_9^{(2)}A^4\cos(4\phi x)\cos(4\psi y) \\ &\quad + \left[M\frac{\partial A}{\partial T_3} - A\chi_3 h(u_c)k_a^2\right]\cos(\phi x)\cos(\psi y), \\ H_2 &= (2\tau A^2 - 2LA^4)b_{21} + (2\tau b_{22}A^2 - 2Lb_{22}A^4)\cos(2\phi x) + (2\tau b_{23}A^2 - 2Lb_{23}A^4)\cos(2\psi y) \\ &\quad + (2\tau b_{24}A^2 - 2Lb_{24}A^4)\cos(2\phi x)\cos(2\psi y) + \frac{\partial A}{\partial T_3}\cos(\phi x)\cos(\psi y), \end{aligned}$$

where

$$\begin{aligned} H_i^{(1)} &= \frac{M\mu}{2u_c}c_{11} + 2\tau b_{1i} \\ &\quad + \frac{1}{2}\left\{2d'(u_c)Mc_{11} - \chi_a h'(u_c)\left(Mc_{21} + c_{11}\right) - \chi_2\left[8h(u_c)b_{2i} + h'(u_c)M\right]\right\}\omega_i^2 \end{aligned}$$

with $i = 1, 2, 3, 4$ and $\omega_1 = 0, \omega_2 = \phi$, $\omega_3 = \psi$, $\omega_4 = k_a$,

$$H_1^{(2)} = \frac{\mu}{2u_c}[(1 + k_a^2)c_{12} + 2b_{11}^2 + b_{12}^2 + b_{13}^2 + \frac{1}{2}b_{14}^2] - 2Lb_{11},$$

and $H_i^{(2)}$ $(i = 2, 3, \cdots, 9)$ are omitted here for brevity. Again, by the solvability condition for Eq. (3.7), i.e. $\langle H, \overline{W}_1\rangle = 0$, it is necessary to let $\chi_3 = 0$ and $T_3 = 0$. Then, using the expression for H, the solution $W_4 = (W_{14}, W_{24})^T$ to Eq. (3.7) can be set as

$$\begin{aligned} W_{i4} = {} & d_{ii}^{(i)}A^2 + d_{ii}^{(2)}A^4 + (d_{i2}^{(i)}A^2 + d_{i2}^{(2)}A^4)\cos(2\phi x) + (d_{i3}^{(i)}A^2 + d_{i3}^{(2)}A^4)\cos(2\psi y) \\ & + (d_{i4}^{(i)}A^2 + d_{i4}^{(2)}A^4)\cos(2\phi x)\cos(2\psi y) + d_{i5}A^4\cos(4\phi x) + d_{i6}A^4\cos(4\psi y) \\ & + d_{i7}A^4\cos(4\phi x)\cos(2\psi y) + d_{i8}A^4\cos(2\phi x)\cos(4\psi y) + d_{i9}A^4\cos(4\phi x)\cos(4\psi y), \end{aligned}$$

where $i = 1, 2$ and the coefficients satisfy

$$\kappa_{i4}(\chi_a)\begin{pmatrix} d_{1i+6} \\ d_{2i+6} \end{pmatrix} = \begin{pmatrix} H_3^{(\frac{1}{2}i+3)} \\ 0 \end{pmatrix}, \ \kappa_{4j}(\chi_a)\begin{pmatrix} d_{1j+5} \\ d_{2j+5} \end{pmatrix} = \begin{pmatrix} H_2^{(\frac{1}{2}j+3)} \\ 0 \end{pmatrix}, \ i = 0, 2, j = 0, 2, 4$$

and

$$\Pi_j(\chi_a)\begin{pmatrix} d_{1j}^{(p)} \\ d_{2j}^{(p)} \end{pmatrix} = \begin{pmatrix} H_j^{(p)} \\ 2(2-p)\tau b_{2j} - 2(p-1)Lb_{2j} \end{pmatrix}, \ p = 1, 2; \ j = 1, 2, 3, 4,$$

where κ_{ij} are defined as in Eq. (A.6) and $\Pi_1 = \kappa_{00}$, $\Pi_2 = \kappa_{20}$, $\Pi_3 = \kappa_{02}$, $\kappa_4 = k_{22}$. Substituting W_1, W_2, W_3, and W_4 into Eq. (3.8) yields

$$I = \left\{\frac{\partial A}{\partial T_4}\rho - \mathbb{I}_1^{(0)}A + \mathbb{I}_1^{(1)}A^3 + \mathbb{I}_1^{(2)}A^5\right\}\cos(\phi x)\cos(\psi y) + \mathbb{I}^*,$$

where $\mathbb{I}_1^{(0)} = \begin{pmatrix} (\chi_2 c_{21} + \chi_4)h(u_c)k_a^2 - \tau c_{11} \\ -\tau c_{21} \end{pmatrix}$, $\mathbb{I}_1^{(1)} = \begin{pmatrix} I_1^{(1)} \\ 3\tau c_{22} - Lc_{21} \end{pmatrix}$, $\mathbb{I}_1^{(2)} = \begin{pmatrix} I_1^{(2)} \\ -3Lc_{22} \end{pmatrix}$, and $\mathbb{I}^* = (I_1^*, I_2^*)^T$ contains automatically orthogonal terms and its explicit expression as well as that of $I_1^{(i)}, i = 1, 2$ are omitted here for brevity. Using the solvability condition for (3.8) once again, we have $\langle I, \overline{W}_1\rangle = 0$, which leads to

$$\frac{\partial A}{\partial T_4} = \widetilde{\tau}A - \widetilde{L}A^3 + \widetilde{Q}A^5, \tag{A.9}$$

where

$$\widetilde{\tau} = \frac{\langle I_1^{(0)}, \overline{\gamma}\rangle}{\langle \gamma, \overline{\gamma}\rangle}, \quad \widetilde{L} = \frac{\langle I_1^{(1)}, \overline{\gamma}\rangle}{\langle \gamma, \overline{\gamma}\rangle}, \quad \widetilde{Q} = -\frac{\langle I_1^{(2)}, \overline{\gamma}\rangle}{\langle \gamma, \overline{\gamma}\rangle}.$$

Taking into account that $\frac{dA}{dt} = \frac{\partial A}{\partial T_1}\varepsilon + \frac{\partial A}{\partial T_2}\varepsilon^2 + \frac{\partial A}{\partial T_3}\varepsilon^3 + \frac{\partial A}{\partial T_4}\varepsilon^4$ with $T_1 = 0$, $T_3 = 0$ and $T_2 = \varepsilon^2 t$, and adding Eqs. (A.9) and (3.12), we obtain the quintic Stuart-Landau equation (3.17) with

$$\overline{\tau} = \tau + \varepsilon^2\widetilde{\tau}, \qquad \overline{L} = L + \varepsilon^2\widetilde{L}, \qquad \overline{Q} = \varepsilon^2\widetilde{Q}. \tag{A.10}$$

Appendix B. Stuart-Landau equation for double eigenvalues

In this appendix we derive the amplitude equations for patterns with double multiplicity, i.e., $p = 2$. Substituting Eq. (3.20) into the linear equation (3.5) yields the following expressions for the components of F:

$$\begin{aligned}
F_1 &= \sum_{i=1}^{2}[\frac{\partial A_i}{\partial T_1}M - \chi_1 h(u_c)k_a^2 A_i]\cos(\xi_i x)\cos(\zeta_i y) \\
&\quad + \sum_{j=1}^{2}\sum_{i=0}^{2} F_i^{(j)} A_j^2 \cos(2\omega_{ij}\Lambda^{(i)}) + \sum_{j=1}^{2} F_3^{(j)} A_j^2 \cos(2\xi_j x)\cos(2\zeta_j y) \\
&\quad + A_1 A_2 \sum_{j=1}^{2}\sum_{i=4}^{5} F_i^{(j)} \cos(\xi_1 + (-1)^i \zeta_2)x \cos(\zeta_1 + (-1)^{j+1}\zeta_2)y, \\
F_2 &= \sum_{i=1}^{2} \frac{\partial A_i}{\partial T_1}\cos(\xi_i x)\cos(\zeta_i y),
\end{aligned}$$

where $\Lambda^{(1)} = x, \Lambda^{(2)} = y$ and

$$F_i^{(j)} = \begin{cases} \dfrac{\mu}{4u_c}M^2 + \dfrac{1}{2}M\left[d'(u_c) - \chi_m h'(u_c)\right]\omega_{ij}^2, & i = 0,1,2,3; j = 1,2, \\ \dfrac{\mu}{2u_c}M^2 + \dfrac{1}{2}M\left[d'(u_c)M - \chi_m h'(u_c)\right]\left[k_a^2 + (-1)^i\xi_1\xi_2 + (-1)^{j+1}\zeta_1\zeta_2\right], & \\ & i = 4,5; j = 1,2 \end{cases}$$

with $\omega_{01} = \omega_{02} = 0$, $\omega_{11} = \xi_1$, $\omega_{21} = \zeta_1$, $\omega_{12} = \xi_2$, $\omega_{22} = \zeta_2$, $\omega_{31} = \omega_{32} = k_a$. In the following two sections we discuss, respectively, the non-resonant and the resonant condition cases.

B.1. The amplitude equation for the non-resonant condition

Suppose that the non-resonant condition (3.21) holds. The solvability condition for Eq. (3.5) leads to $\chi_1 = 0$ and $T_1 = 0$. Then, the solution of Eq. (3.5) can be set as

$$\begin{aligned}
W_{i2} &= A_1^2 b_{i1}^{(1)} + A_2^2 b_{i1}^{(2)} + A_1^2 b_{i2}^{(1)}\cos(2\xi_1 x) + A_2^2 b_{i2}^{(2)}\cos(2\xi_2 x) + A_1^2 b_{i3}^{(1)}\cos(2\zeta_1 y) \\
&\quad + A_2^2 b_{i3}^{(2)}\cos(2\zeta_2 y) + A_1^2 b_{i4}^{(1)}\cos(2\xi_1 x)\cos(2\zeta_1 y) + A_2^2 b_{i4}^{(2)}\cos(2\xi_2 x)\cos(2\zeta_2 y) \\
&\quad + b_{i5}A_1A_2\cos(\xi_1+\xi_2)x\cos(\zeta_1+\zeta_2)y + b_{i6}A_1A_2\cos(\xi_1+\xi_2)x\cos(\zeta_1-\zeta_2)y \\
&\quad + b_{i7}A_1A_2\cos(\xi_1-\xi_2)x\cos(\zeta_1+\zeta_2)y + b_{i8}A_1A_2\cos(\xi_1-\xi_2)x\cos(\zeta_1-\zeta_2)y
\end{aligned} \tag{B.1}$$

with $i = 1, 2$ and the coefficients satisfying

$$\mathbb{B}_{4\omega_{ij}^2}(\chi_a)\begin{pmatrix} b_{1(i+1)}^{(j)} \\ b_{2(i+1)}^{(j)} \end{pmatrix} = \begin{pmatrix} F_i^{(j)} \\ 0 \end{pmatrix}, \quad i = 0,1,2,3;\ j = 1,2$$

with

$$\mathbb{B}_{[\xi_1+(-1)^i\xi_2]^2+[\zeta_1+(-1)^{j+1}\zeta_2]^2}(\chi_a)\begin{pmatrix} b_{1(2i+j-4)} \\ b_{2(2i+j-4)} \end{pmatrix} = \begin{pmatrix} F_i^{(j)} \\ 0 \end{pmatrix},\ i = 4,5;\ j = 1,2,$$

where

$$\mathbb{B}_\vartheta(\chi_a) = \begin{pmatrix} -\vartheta d(u_c) - \mu & \chi_a h(u_c)\vartheta \\ 1 & -\vartheta - 1 \end{pmatrix}. \tag{B.2}$$

Plugging Eq. (B.1) into Eq. (3.6) results in the following expression for $G = (G_1, G_2)$:

$$\begin{aligned} G_1 &= \left[\frac{\partial A_1}{\partial T_2} M - G_1^{[0]} A_1 + G_1^{[1]} A_1^3 + G_1^{[2]} A_1 A_2^2\right] \cos(\xi_1 x)\cos(\zeta_1 y) \\ &\quad + \left[\frac{\partial A_2}{\partial T_2} M - G_1^{[0]} A_2 + G_1^{[3]} A_2^3 + G_1^{[4]} A_2 A_1^2\right] \cos(\xi_2 x)\cos(\zeta_2 y) + G_1^*, \\ G_2 &= \frac{\partial A_1}{\partial T_2}\cos(\xi_1 x)\cos(\zeta_1 y) + \frac{\partial A_2}{\partial T_2}\cos(\xi_2 x)\cos(\zeta_2 y) + G_2^*, \end{aligned}$$

where $G_1^{[0]} = k_a^2 \chi_2 h(u_c)$, both G_1^* and G_2^* contain automatically orthogonal terms and their explicit expressions are omitted here for brevity; the remaining coefficients have three different expressions corresponding to three cases as follows:

Case (I): both ξ_i and ζ_i, $i = 1, 2$ are not equal to zero. In this case, we have

$$G_1^{[1]} = G_1^{(1)1}, \quad G_1^{[2]} = G_1^{(2)1}, \quad G_1^{[3]} = G_1^{(3)2}, \quad G_1^{[4]} = G_1^{(4)2}$$

with

$$\begin{aligned} G_1^{(i)j}|_{(i=2j-1;j=1,2)} &= \frac{1}{4}\left(\frac{2\mu}{u_c} + d'(u_c)k_a^2\right) M \left(2b_{12}^{(j)} + 4b_{11}^{(j)} + 2b_{13}^{(j)} + b_{14}^{(j)}\right) + \frac{3}{32} d''(u_c) M^3 k_a^2 \\ &\quad - \chi_a h'(u_c)\left[M\left(b_{22}^{(j)}\omega_{1j}^2 + b_{23}^{(j)}\omega_{2j}^2 + \frac{1}{2} b_{24}^{(j)} k_a^2\right) + \left(b_{11}^{(j)} - \frac{1}{4} b_{14}^{(j)}\right) k_a^2 \right. \\ &\quad \left. + \frac{1}{2}\left(\omega_{2j}^2 - \omega_{1j}^2\right)\left(b_{12}^{(j)} - b_{13}^{(j)}\right)\right] - \frac{3}{32}\chi_a h''(u_c) M^2 k_a^2, \\ G_1^{(i)j}|_{(i=2j;j=1,2)} &= \left(\frac{2\mu}{u_c} + d'(u_c)k_a^2\right) M \left(b_{11}^{(3-j)} + \frac{1}{4}\sum_{m=5}^{8} b_{1m}\right) + \frac{3}{8} d''(u_c) M^3 k_a^2 \\ &\quad - \frac{1}{4}\chi_a h'(u_c)\left[M k_a^2 \sum_{m=5}^{8} b_{2m} + (\phi_1\phi_2 + \psi_1\psi_2)\left[M(b_{25} - b_{28}) + b_{18} - b_{15}\right]\right. \\ &\quad \left. + (\phi_1\phi_2 - \psi_1\psi_2)\left[M(b_{26} - b_{27}) + b_{17} - b_{16}\right] + 4b_{11}^{(3-j)} k_a^2\right] \\ &\quad - \frac{3}{8}\chi_a h''(u_c) M^2 k_a^2. \end{aligned}$$

Case (II): only one of ξ_1, ζ_1, ξ_2 and ζ_2 is zero. Without loss of generality, suppose $\xi_1 = 0$, then $k_a^2 = \xi_2^2 + \zeta_2^2 = \zeta_1^2$, and

$$G_1^{[1]} = G_1^{(1)1} + G_1^{(9)1}, \quad G_1^{[2]} = G_1^{(2)1}, \quad G_1^{[3]} = G_1^{(3)2}, \quad G_1^{[4]} = G_1^{(4)2} + G_1^{(10)2}$$

with $G_1^{(9)1} = G_1^{(5)1}$, and

$$G_1^{(10)2} = \left(\frac{2\mu}{u_c} + d'(u_c)k_a^2\right) M \left(b_{12}^{(1)} + \frac{1}{4}\sum_{m=5}^{8} b_{1m}\right) + \frac{1}{8} d''(u_c) M^3 k_a^2 - \frac{1}{8}\chi_a h''(u_c) M^2 k_a^2$$

$$-\frac{1}{4}\chi_a h'(u_c)\Big[Mk_a^2\sum_{m=5}^{8}b_{2m}+\zeta_1\zeta_2[M(b_{25}+b_{27}-b_{26}-b_{28})$$
$$+b_{16}+b_{18}-b_{15}-b_{17}]+4b_{12}^{(1)}k_a^2\Big].$$

Case (III): only one of the relations $\xi_1=\zeta_2=0$ and $\xi_2=\zeta_1=0$ is satisfied. Without loss of generality, we assume that $\xi_1=\zeta_2=0$. Then $k_a^2=\xi_2^2=\zeta_1^2$, and

$$G_1^{[1]}=G_1^{(1)1}+G_1^{(5)1},\quad G_1^{[2]}=G_1^{(2)1}+G_1^{(6)1},\quad G_1^{[3]}=G_1^{(3)2}+G_1^{(7)2},\quad G_1^{[4]}=G_1^{(4)2}+G_1^{(8)2}$$

with

$$\begin{aligned}G_1^{(i)j}|_{(i=2j+3;j=1,2)}&=\frac{1}{4}\left(\frac{2\mu}{u_c}+d'(u_c)k_a^2\right)M\left(2b_{1(j+1)}^{(j)}+b_{14}^{(j)}\right)+\frac{1}{32}d''(u_c)M^3k_a^2\\&\quad-\frac{1}{2}\chi_a h'(u_c)\omega_{(3-j)j}^2\left[Mb_{24}^{(j)}+b_{1(j+1)}^{(j)}-\frac{1}{2}b_{14}^{(j)}\right]-\frac{1}{32}\chi_a h''(u_c)M^2k_a^2,\\G_1^{(i)j}|_{(i=2j+4;j=1,2)}&=\frac{1}{4}\left(\frac{2\mu}{u_c}+d'(u_c)k_a^2\right)M\left(4b_{1(4-j)}^{(3-j)}+\sum_{m=5}^{8}b_{1m}\right)+\frac{1}{8}d''(u_c)M^3k_a^2\\&\quad-\frac{1}{4}\chi_a h'(u_c)\omega_{(3-j)j}^2\left[M\sum_{m=5}^{8}b_{2m}+4b_{1(4-j)}^{(3-j)}\right]-\frac{1}{8}\chi_a h''(u_c)M^2k_a^2.\end{aligned}$$

Then, by the solvability condition for Eq. (3.6), we obtain the coupled Landau equations (3.23) for the amplitudes A_1 and A_2. The coefficients in Eq. (3.23) are expressed by

$$\tau=\frac{MG_1^{[0]}}{\langle\gamma,\overline{\gamma}\rangle}=\frac{Mk_a^2\chi_2h(u_c)}{M^2+\chi_a h(u_c)k_a^2},\quad L_j=\frac{MG_1^{(2j-1)j}}{\langle\gamma,\overline{\gamma}\rangle}+L_j^*,\quad \Omega_j=-\frac{MG_1^{(2j)j}}{\langle\gamma,\overline{\gamma}\rangle}+\Omega_j^*,\ j=1,2.$$

For case (I) the coefficients $L_j^*=0$ and $\Omega_j^*=0$. On the other hand, for case (II), $\Omega_1^*=0$ and $L_2^*=0$, while L_1^* and Ω_2^* are given as

$$L_1^*=\frac{MG_1^{(9)1}}{\langle\gamma,\overline{\gamma}\rangle}=\frac{MG_1^{(9)1}}{M^2+\chi_a h(u_c)k_a^2},\qquad \Omega_2^*=\frac{-MG_1^{(10)2}}{\langle\gamma,\overline{\gamma}\rangle}=\frac{-MG_1^{(10)2}}{M^2+\chi_a h(u_c)k_a^2}.\tag{B.3}$$

Finally, for case (III), the coefficient L_1^* is the same as that in Eq. (B.3) and the expressions for L_2^* and Ω_j^* are:

$$L_2^*=\frac{MG_1^{(7)2}}{\langle\gamma,\overline{\gamma}\rangle}=\frac{MG_1^{(7)2}}{M^2+\chi_a h(u_c)k_a^2},\qquad \Omega_j^*=\frac{-MG_1^{(2j+4)j}}{\langle\gamma,\overline{\gamma}\rangle}=\frac{-MG_1^{(2j+4)j}}{M^2+\chi_a h(u_c)k_a^2}.$$

B.2. The amplitude equation for the resonant condition

Substituting Eq. (3.32) into the system (3.5) yields the following new expressions for the components of F:

$$\begin{aligned}F_1&=\sum_{i=1}^{2}\left[\frac{\partial A_i}{\partial T_1}M-F_1^{(0)}A_i+i^2F_2^{(2)}A_1^{i-1}A_2^{3-i}\right]\cos(\xi_i x)\cos(\zeta_i y)\\&\quad+\sum_{i=1}^{2}\left[\frac{\mu}{4u_c}M^2+(2-i)F_1^{(1)}\right]A_i^2+\sum_{i=1}^{2}\left[iF_i^{(3-i)}A_{3-i}^2\cos\left(2\omega_{i(3-i)}\Lambda^{(i)}\right)\right.\end{aligned}$$

$$+ (3-i)^2 F_i^{(3-i)} A_1^{2-i} A_2^i \cos(i\xi_2 x)\cos\left((4-i)\zeta_2 y\right)\Bigg],$$

$$F_2 = \sum_{i=1}^{2} \frac{\partial A_i}{\partial T_1}\cos(\xi_i x)\cos(\zeta_i y),$$

where $F_1^{(0)} = \chi_1 h(u_c)k_a^2$, $\Lambda^{(1)} = x$ and $\Lambda^{(2)} = y$. By applying the solvability condition for Eq. (3.7), i.e., $\langle F, \overline{W}_1\rangle = 0$, we obtain the system (3.33) with

$$\tau = \frac{F_1^{(0)} M}{\langle \gamma, \overline{\gamma}\rangle} = \frac{\chi_1 h(u_c)k_a^2 M}{M^2 + \chi_m h(u_c)k_a^2}, \qquad L = \frac{4F_2^{(2)} M}{\langle \gamma, \overline{\gamma}\rangle} = \frac{4F_2^{(2)} M}{M^2 + \chi_m h(u_c)k_a^2}.$$

However, Eq. (3.33) cannot capture the amplitude of the stationary pattern. To proceed, using Eq. (3.33) in the expressions for F_1 and F_2 yields

$$\begin{aligned}
F_1 = \sum_{i=1}^{2} \Bigg[& [(\tau - F_1^{(0)})A_i + i^2(F_2^{(2)} - \frac{L}{4}M)A_1^{i-1}A_2^{3-i}]\cos(\xi_i x)\cos(\zeta_i y) \\
& + \left[(2-i)F_1^{(1)} + \frac{\mu}{4u_c}M^2\right] A_i^2 + iF_i^{(3-i)} A_{3-i}^2 \cos\left(2\omega_{i(3-i)}\Lambda^{(i)}\right) \\
& + (3-i)^2 F_i^{(3-i)} A_1^{2-i} A_2^i \cos(i\xi_2 x)\cos((4-i)\zeta_2 y)\Bigg],
\end{aligned}$$

$$F_2 = \sum_{i=1}^{2} i^2 \left(F_2^{(2)} - \frac{L}{4}M\right) A_1^{i-1} A_2^{3-i}\cos(\xi_i x)\cos(\zeta_i y).$$

Then, we obtain the expression for $W_2 = (W_{12}, W_{22})$ as

$$\begin{aligned}
W_{i2} = {} & A_1^2 b_{i3}^{(1)} + A_2^2 b_{i3}^{(2)} + (A_1 b_{i1}^{(1)} + A_2^2 b_{i1}^{(2)})\cos(2\zeta_2 y) + A_1^2 b_{i4}^{(1)}\cos(4\zeta_2 y) \\
& + A_2^2 b_{i5}^{(1)}\cos(2\sqrt{3}\zeta_2 x) + (A_2 b_{i2}^{(1)} + A_1 A_2 b_{i2}^{(2)})\cos(\sqrt{3}\zeta_2 x)\cos(\zeta_2 y) \\
& + A_1 A_2 b_{i7}^{(1)}\cos(\sqrt{3}\zeta_2 x)\cos(3\zeta_2 y) + A_2^2 b_{i6}^{(1)}\cos(2\sqrt{3}\zeta_2 x)\cos(2\zeta_2 y),
\end{aligned} \tag{B.4}$$

where $i = 1, 2$ and the coefficients satisfy

$$\begin{aligned}
& \mathbb{B}_{k_a^2}(\chi_a)(b_{1j}^{(p)}, b_{2j}^{(p)})^T \\
& = \left((2-p)(\tau M - \chi_1 h(u_c)k_a^2 + (p-1)j^2(F_2^{(2)} - \frac{L}{4}M), (2-p)\tau + (p-1)j^2(-\frac{L}{4})\right)^T
\end{aligned}$$

with $j = 1, 2$ and $p = 1, 2$;

$$\mathbb{B}_{4k_a^2}(\chi_a)(b_{1j}^{(1)}, b_{2j}^{(1)})^T = \left((4 - \frac{1}{2}j)F_2^{(1)}, 0\right)^T, \ j = 4, 6;$$

$$\mathbb{B}_{3k_a^2}(\chi_a)(b_{1j}^{(1)}, b_{2j}^{(1)})^T = \left((\frac{3}{2}j - \frac{13}{2})F_1^{(2)}, 0\right)^T, j = 5, 7;$$

$$\mathbb{B}_0(\chi_a)(b_{13}^{(p)}, b_{23}^{(p)})^T = \left(\frac{\mu}{4u_c}M^2 + (2-p)F_1^{(1)}, 0\right)^T, \ p = 1, 2,$$

and $\mathbb{B}_{k_a^2}$ defined in Eq. (B.2). Now, substituting W_1 and W_2 into Eq. (3.6) yields

$$G = \sum_{j=1}^{2} \left[\frac{\partial A_j}{T_2}\rho + G_j^{(1)} A_j + G_j^{(2)} A_1^{j-1} A_2^{3-j} + G_j^{(3)} A_1^j A_2^{3-j} + G_j^{(4)} A_j^3 \right] \cos(\xi_j x)\cos(\zeta_j y) + G^*,$$

where $G^* = (G_1^*, G_2^*)$ defined as in (B.1), $G_j^{(i)} = (G_{1j}^{(i)},\ G_{2j}^{(i)})^T,\ i = 1,2,3,4$ with

$$G_{2j}^{(1)} = \tau b_{2j}^{(1)}, \quad G_{2j}^{(2)} = 2\tau b_{2j}^{(2)} - \frac{j^2}{4} L b_{2j}^{(1)}, \quad G_{2j}^{(3)} = -(3-j) L b_{2j}^{(2)}, \quad G_{2j}^{(4)} = -\frac{j-1}{4} L b_{2j}^{(2)}$$

and

$$G_{1j}^{(1)} = \tau b_{11}^{(1)} - \chi_1 h(u_c) b_{21}^{(1)} k_a^2 - \chi_2 h(u_c) k_a^2, j = 1,2,$$

$G_{11}^{(i)}$ and $G_{12}^{(i)}, i = 2,3,4$ are omitted here for brevity.

Once again, the solvability condition $\langle G, \overline{W}_1 \rangle = 0$ results in the following amplitude equations for A_1 and A_2:

$$\begin{cases} \dfrac{\partial A_1}{\partial T_2} &= \tilde{\tau}_1 A_1 - \tilde{L}_1 A_2^2 + \tilde{\Omega}_1 A_1 A_2^2 + \tilde{\Psi}_1 A_1^3, \\ \dfrac{\partial A_2}{\partial T_2} &= \tilde{\tau}_2 A_2 - \tilde{L}_2 A_1 A_2 + \tilde{\Omega}_1 A_1^2 A_2 + \tilde{\Psi}_1 A_2^3 \end{cases} \tag{B.5}$$

with

$$\tilde{\tau}_j = -\frac{\langle G_j^{(1)}, \overline{\gamma} \rangle}{\langle \gamma, \overline{\gamma} \rangle},\ \tilde{L}_j = \frac{\langle G_j^{(2)}, \overline{\gamma} \rangle}{\langle \gamma, \overline{\gamma} \rangle},\ \tilde{\Omega}_1 = -\frac{\langle G_j^{(3)}, \overline{\gamma} \rangle}{\langle \gamma, \overline{\gamma} \rangle} \tilde{\Psi}_1 = -\frac{\langle G_j^{(4)}, \overline{\gamma} \rangle}{\langle \gamma, \overline{\gamma} \rangle},\ j = 1,2.$$

Together with the system (3.33), by a simple computation, Eq. (B.5) yields the cubic Stuart-Landau equation (3.34) whose coefficients satisfy

$$\bar{\tau}_j = \varepsilon\tau + \varepsilon^2 \tilde{\tau}_j, \quad \bar{L}_1 = \frac{L}{4}\varepsilon + \varepsilon^2 \tilde{L}_j, \quad \bar{\Omega}_j = \varepsilon^2 \tilde{\Omega}_j, \quad \bar{\Psi}_j = \varepsilon^2 \bar{\Psi}_1, \quad j = 1,2.$$

References

[1] G. Gambino, M.C. Lombardo, M. Sammartino, Turing instability and traveling fronts for a nonlinear reaction-diffusion system with cross-diffusion, Math. Comput. Simulation 82 (2012) 1112–1132.

[2] G. Gambino, M.C. Lombardo, M. Sammartino, Pattern formation driven by cross-diffusion in a 2D domain, Nonlinear Anal. Real World Appl. 14 (2013) 1755–1779.

[3] G. Gambino, M.C. Lombardo, M. Sammartino, V. Sciacca, Turing pattern formation in the Brusselator system with nonlinear diffusion, Phys. Rev. E 88 (2013) 042925.

[4] G. Gambino, M.C. Lombardo, M. Sammartino, Turing instability and pattern formation for the Lengyel-Epstein system with nonlinear diffusion, Acta Appl. Math. 132 (2014) 283–294.

[5] M. Ghergu, Non-constant steady-state solutions for Brusselator type systems, Nonlinearity 21 (2008) 2331–2345.

[6] D. Iron, M.J. Ward, J.C. Wei, The stability of spike solutions to the one-dimensional Gierer-Meinhardt model, Phys. D 150 (1–2) (2001) 25–62.

[7] L. Jin, Q. Wang, Z. Zhang, Pattern formation in Keller-Segel chemotaxis models with logistic growth, Internat. J. Bifur. Chaos 26 (2) (2016) 1650033.

[8] C.T. Kelley, Solving Nonlinear Equations with Newton's Method, SIAM, 2003.

[9] K. Kuto, K. Osaki, T. Sakurai, T. Tsujikawa, Spatial pattern formation in a chemotaxis-diffusion growth model, Phys. D (2012).

[10] G.M. Lieberman, Bounds for the steady-state Sel'kov model for arbitrary p in any number of dimensions, SIAM J. Math. Anal. 36 (5) (2005) 1400–1406.

[11] M. Ma, Z.A. Wang, Global bifurcation and stability of steady states for a reaction-diffusion-chemotaxis model with volume-filling effect, Nonlinearity 28 (2015) 2639–2660.

[12] M. Ma, Z.A. Wang, Patterns in a generalized volume-filling chemotaxis model with cell proliferation, Anal. Appl. 15 (2017) 83–106.

[13] M. Ma, C.H. Ou, Z.A. Wang, Stationary solutions of a volume-filling chemotaxis model with logistic growth and their stability, SIAM J. Appl. Math. 72 (2012) 740–766.
[14] M. Ma, M.Y. Gao, C.Q. Tong, Y.Z. Han, Chemotaxis-driven pattern formation for a reaction-diffusion-chemotaxis model with volume-filling effect, Comput. Math. Appl. 72 (2016) 1320–1340.
[15] M.-J. Ma, H. Li, M.Y. Gao, J.C. Tao, Y.Z. Han, Traveling wavefronts for a reaction-diffusion-chemotaxis model with volume-filling effect, Appl. Math. J. Chinese Univ. 32 (1) (2017) 108–116.
[16] K.J. Painter, T. Hillen, Volume-filling and quorum-sensing in models for chemosensitive movement, Can. Appl. Math. Q. 10 (2002) 501–543.
[17] K.J. Painter, T. Hillen, Spatio-temporal chaos in a chemotaxis model, Phys. D 240 (2011) 363–375.
[18] P.Y.H. Pang, M.X. Wang, Strategy and stationary pattern in a three-species predator-prey model, J. Differential Equations 200 (2004) 245–274.
[19] J. Shi, X. Wang, On global bifurcation for quasilinear elliptic systems on bounded domains, J. Differential Equations 246 (2009) 2788–2812.
[20] A. Turing, The chemical basis of morphogenesis, Philos. Trans. R. Soc. B 237 (1957) 37–72.
[21] M.X. Wang, Non-constant positive steady states of the Sel'kov model, J. Differential Equations 190 (2) (2003) 600–620.
[22] Q. Wang, J. Yan, C. Gai, Qualitative analysis of stationary Keller-Segel chemotaxis models with logistic growth, Z. Angew. Math. Phys. 67 (3) (2016) 51.
[23] Q. Wang, J. Yang, L. Zhang, Time periodic and stable patterns of a two-competing-species Keller-Segel chemotaxis model: effect of cellular growth, Discrete Contin. Dyn. Syst. Ser. B 22 (9) (2017) 3547–3574.
[24] Z.A. Wang, On chemotaxis models with cell population interactions, Math. Model. Nat. Phenom. 5 (2010) 173–190.
[25] Z.A. Wang, T. Hillen, Classical solutions and pattern formation for a volume filling chemotaxis model, Chaos 17 (2007) 037108.
[26] Z.A. Wang, M. Winkler, D. Wrzosek, Global regularity versus infinite-time singularity formation in a chemotaxis model with volume filling effect and degenerate diffusion, SIAM J. Math. Anal. 44 (2012) 3502–3525.